VANADATE-PHOSPHATE SUBSTITUTIONAL STUDIES

CATION SUBSTITUTION STUDIES

IN

SOME VANADATE-PHOSPHATE SYSTEMS

By

KATHLEEN LORALEE IDLER

A Thesis

Submitted to the School of Graduate Studies

in Partial Fulfilment of the Requirements

for the Degree

Master of Science

McMaster University

September, 1977

TO FATHER

MASTER OF SCIENCE (1977) McMASTER UNIVERSITY
(Chemistry) Hamilton, Ontario

TITLE: Cation Substitution Studies in Some Vanadate-Phosphate Systems

AUTHOR: Kathleen Loralee Idler, B.Sc. (U.B.C.)

SUPERVISORS: Dr. C. Calvo and Dr. H.N. Ng

NUMBER OF PAGES: x, 95

ABSTRACT

Cation substitution studies in several vanadate-phosphate systems have revealed substantial substitution between pentavalent V and P in tetrahedral sites in both ring and chain structures. The phase $Zn_3V_{0.5}P_{1.5}O_8$ has been prepared and its structure has been determined and found to be similar to that of α-$Zn_3(PO_4)_2$. It crystallizes in the space group C2/c with rings of $Zn(1)O_4$ and $(V,P)O_4$ tetrahedra sharing corners to form chains, which are linked to neighbouring chains by $Zn(2)O_4$ tetrahedra. The edge-sharing between Zn tetrahedra which is found in α-$Zn_3(PO_4)_2$ is absent in $Zn_3V_{0.5}P_{1.5}O_8$. There is no evidence of long-range ordering of V^{5+} and P^{5+} cations in this structure.

Three pyroxene-like phases, related to $NaVO_3$ and characterized by tetrahedral chains, have been prepared. The $NaV_{2/3}P_{1/3}O_3$ structure closely resembles that of $NaVO_3$, and shows no long-range ordering of V^{5+} and P^{5+}. The mixed phases $Na_{.875}K_{.125}VO_3$ and $Na_{0.5}K_{0.5}VO_3$ were prepared in order to study the effects of M^+ substitution on the $NaVO_3$ structure. The structure of $Na_{.875}K_{.125}VO_3$ resembles that of $NaVO_3$ and $NaV_{2/3}P_{1/3}O_3$, while $Na_{0.5}K_{0.5}VO_3$ has the true diopside structure, with Na and K ordered in two nonequivalent sites. All three structures were refined in the space group C2/c and the effects of cation substitution on the configuration of the tetrahedral chains are discussed.

ACKNOWLEDGEMENTS

I wish to express my gratitude to the late Dr. Crispin Calvo, who was not only a conscientious supervisor and a dedicated scientist, but also an outstanding example of courage and grace under pressure. I would like to thank Dr. J.A. Morrison, who kept things running smoothly, and Dr. H.N. Ng, for his invaluable assistance and advice. I would also like to thank the faculty members and graduate students in the Crystallography group for many useful discussions, J.D. Garrett and R. Faggiani for their technical assistance, and Mrs. Pauline Horridge for typing and correcting the manuscript.

I would like to thank the Government of the Province of Ontario and the Department of Chemistry of McMaster University for their financial assistance.

TABLE OF CONTENTS

LIST OF TABLES

LIST OF FIGURES

CHAPTER I

INTRODUCTION

1.1 Scope of Work

Vanadium V is known to assume both tetrahedral and distorted octahedral coordination. Mixed oxides of the type $nMO:V_2O_5$ have been extensively studied. The vanadium is octahedrally coordinated when the ratio of divalent metal oxide to V_2O_5 is 1:1, and is tetrahedrally coordinated when the ratio is greater than one. Isomorphism between the arsenates and vanadates is common, but it is very rare between phosphates and either vanadates and/or arsenates. The graftonite structure type (Calvo, 1968b) has been found to be common to the phosphates and the vanadates and/or the arsenates, and $\beta_{II}Li_3VO_4$, which has an ordered wurtzite structure (Shannon and Calvo, 1973b) is isotypic with that of $\beta_{II}Li_3PO_4$ (Tarte, 1967). Therefore, substitution of V^{5+} for P^{5+} in tetrahedral sites, although possible, rarely occurs over a wide composition range. Brixner, Flippen and Jeitschko (1975) found limited substitution of the pentavalent ion at either end of the $Pb_3(PO_4)_2$-$Pb_3(VO_4)_2$ join, but they have not reported the structures of the solid solutions. There is also some evidence of limited solubility of excess vanadium in tetrahedral P^{5+} sites in both α-VPO_5 (Jordan and Calvo, 1973) and βVPO_5 (Gopal and Calvo, 1972) where the V^{5+} environment is a highly distorted octahedron with one long and one short axial V-O bond. In view of the lack of structural similarities between phosphates and vanadates, mixed phases containing tetrahedral V/P are expected to adopt structure types

different from those of their end members.

Two systems, one showing substantial substitution of V^{5+} for P^{5+}, and the other showing substitution of P^{5+} for V^{5+} have been chosen for study in this work.

The first system is $Zn_3(V,P)_2O_8$ and the second system is $Na(V,P)O_3$. Metal cation substitution in the latter system was also studied for reasons which will be discussed later.

1.2 The $Zn_3(V,P)_2O_8$ System

The phase relationships and luminescence of several compounds with the stoichiometry $M_3P_2O_8$ have been extensively studied. The crystal structures of several mixed phases have been determined, but with emphasis on M^{2+} substitution. In their study of the $Zn_3(PO_4)_2$-$Zn_3(VO_4)_2$ join, Brown and Hummel (1965) found a solid solution stable between 18 and 28 mole percent $Zn_3(VO_4)_2$ and below 835°C. The simplest molar ratios in this region are $15ZnO:4P_2O_5:V_2O_5$ and $12ZnO:3P_2O_5:V_2O_5$. The latter phase, hereafter referred to as $Zn_3V_{0.5}P_{1.5}O_8$, has been prepared and its crystal structure determined during the course of this work.

The purpose of this structure determination is two-fold: firstly, to discover if the structure adopted by the mixed phase is new or previously known; and secondly, to determine whether the distribution of V and P is random or ordered.

1.3 The $(Na,K)(P,V)O_3$ System

1.3.1 The pyroxene structures

The alkali metal metavanadates are structurally related to the group of minerals known as pyroxenes, which are chain silicates with

the general formula $M1M2X_2O_6$. In nature, X = Si^{4+}, M1 = Mg^{2+}, Fe^{2+}, Fe^{3+}, Mn^{2+}, Al^{3+} and M2 = Ca^{2+}, Mg^{2+}, Fe^{2+}, Mn^{2+}, Na^{+} and Li^{+}. They comprise the most important group of rock forming ferromagnesium silicates (Deer, Howie and Zussman, 1963) and are commonly found in lunar rocks. This accounts for the considerable interest which geologists have shown in these systems in recent years. The first pyroxene structure, that of diopside ($CaMgSi_2O_6$), was determined by Warren and Bragg in 1929. In the past ten years, a large number of pyroxene structures have been determined (for a review, see, for example, Papike, Prewitt, Sueno and Cameron, 1973).

In nature, the most common pyroxenes are found in the ternary system $MgSiO_3$-$FeSiO_3$-$CaSiO_3$ (Figure 1.1), and they fall into two classes; the orthorhombic or orthopyroxenes, which are only found near the $MgSiO_3$-$FeSiO_3$ join, and the monoclinic or clinopyroxenes, with which this work is solely concerned. The prototype structure for the clinopyroxenes is that of diopside. It contains SiO_4 tetrahedra, which share corners to form a single type of chain running parallel to the c-axis (Figure 4.2). Chains separated by half of b form layers parallel to (100). These layers are separated by one-half a, and the metal cations M1 and M2 form layers sandwiched between them. Using the nomenclature of Burnham, Clark, Papike and Prewitt (1967), the smaller, approximately octahedral sites are labelled M1, and the larger, more irregular sites are labelled M2. In diopside, the M2 site is occupied by Ca^{2+} and is eight-fold coordinated. The bridging oxygen in the Si-O chain is labelled O3 and the non-bridging oxygens are called O1 and O2. The M1 octahedra share edges to form chains parallel to c. Each M2 polyhedron shares edges with three adjacent M1

Figure 1.1 Occurrence of Silicate Clinopyroxenes

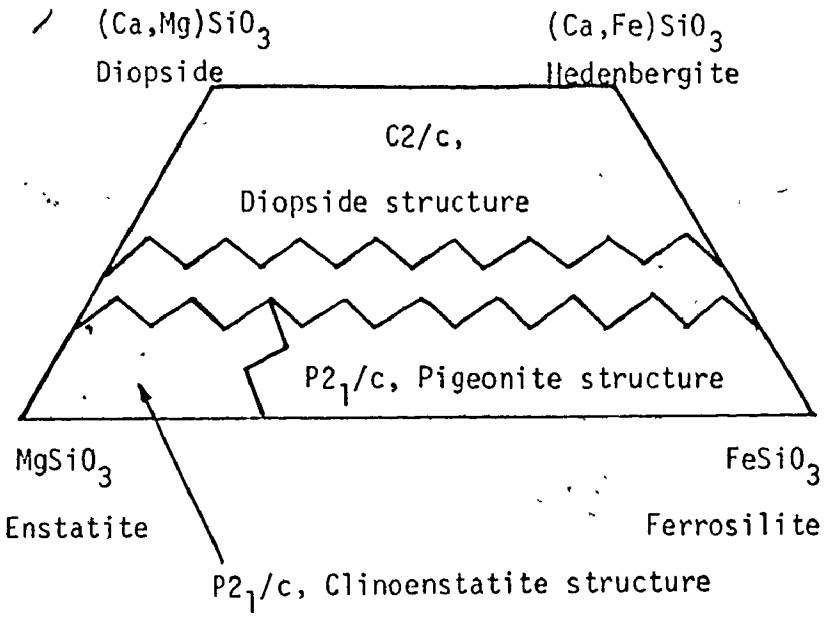
(Ca,Mg)SiO3
Diopside
(Ca,Fe)SiO3
Hedenbergite
C2/c,
Diopside structure
P21/c, Pigeonite structure
MgSiO3
Enstatite
FeSiO3
Ferrosilite
P21/c, Clinoenstatite structure

octahedra located in the same chain.

The space groups so far observed for clinopyroxenes are C2/c, C2, $P2_1/c$, and P2. Starting from the prototype C2/c diopside structure, the pyroxene structures can vary in one of several ways with cation substitution. Substitution may result in a change in unit cell parameters and some distortion or displacement of the silicate chains without altering the space group symmetry. Substitutions in the diopside-hedenbergite ($CaFeSi_2O_6$) series fall into this category. Distortions of the silicate chain to accomodate small cations may result in the production of two types of tetrahedra and reduction in the space group symmetry. Spodumene ($LiAlSi_2O_6$), which is reported to have space group C2 (Clark, Appleman and Papike, 1969) is an example of this. Small cations on the M2 site can result in displacement of the metal ions from the diads, with the production of two types of silicate chains as a result. Clinoenstatite ($MgSiO_3$) is an example of this, having the space group $P2_1/c$, and a six-fold coordinated M2 site (Morimoto, Appleman and Evans, 1960).

1.3.2 Previous work on metavanadate clinopyroxenes

Prior to this work, two alkali metal metavanadates were found to adopt clinopyroxene structures. These were $NaVO_3$ (Prewitt et al., 1972, and Marumo et al., 1974) and $LiVO_3$ (Shannon and Calvo, 1973a). A number of other metavanadates: KVO_3, NH_4VO_3, $RbVO_3$, $CsVO_3$ (Hawthorne and Calvo, 1977) and $TlVO_3$ (Ganne et al., 1974) were found to be orthorhombic, with space group Pbcm. Both $LiVO_3$ and $NaVO_3$ have been refined in space group C2/c, and both space group assignments have been questioned. Reflections in violation of the c glide symmetry have been noted in the

case of $LiVO_3$ (Shannon and Calvo, 1973). Similar violations were found in the case of spodumene (Clark, Appleman and Papike, 1969). These authors claim that only those pyroxenes in which M2 is eight-fold coordinated have the C2/c structure, and that all pyroxenes with six-fold coordinated M2 sites have different space groups. However, the refinement of spodumene in C2/c is almost identical to those of "true" C2/c pyroxenes. Positional disorder of the Li^+ ion has been proposed to account for the space group violation in $LiVO_3$ (Shannon and Calvo, 1973).

The structure of $NaVO_3$ has been refined by Prewitt et al. (1972) and Marumo et al. (1974) in the space group C2/c. It has essentially the diopside structure with both M1 and M2 sites six-coordinated. Ramani et al. (1975) refined the structure at 550°C in space group C2/c, but chose the space group Cc for the room temperature structure because of the reported ferroelectric behaviour of $NaVO_3$ below 380°C (Sawada and Nomura, 1951). They found no significant changes in the atomic positions from room temperature to 550°C. There are some discrepancies in the lattice parameters reported by these authors. They are listed in Table 1.1 together with those measured in the present work.

There would seem to be some doubt that the room temperature phase of $NaVO_3$ is ferroelectric. Although the domain structure and hysteresis loop characteristic of ferroelectric materials were observed, the loop flattens near room temperature and the application of electric fields and mechanical stress has no effect on the domain structure (Sawada and Nomura, 1951). The dielectric anomaly near the Curie point at 400°C was not reproducible (Matsuda, 1974).

Table 1.1

$NaVO_3$ Unit Cell Parameters

	Source				
	This work	Marumo et al. (1974)	Prewitt et al. (1972)	Ramani et al. (1975)	
				25°C	550°C
a(Å)	10.538(9)	10.552(3)	10.559(4)	10.494(9)	10.595(15)
b(Å)	9.444(7)	9.468(2)	9.466(3)	9.434(7)	9.671(10)
c(Å)	5.865(2)	5.879(2)	5.877(2)	5.863(6)	5.926(8)
β(°)	108.42(5)	108.47(3)	108.49(3)	108.80	108.75
space group	C2/c	C2/c	C2/c	Cc	C2/c

Some cation substitution in $NaVO_3$ has been reported. In their study of the $NaVO_3$-$NaPO_3$ join, Bergman and Sanzharova (1970) indicated no compound or solid solution formation. However, Ohashi (1964) reported the existence of some mixed phases. Perraud (1974), in his study of the $NaVO_3$-KVO_3 join, reported the existence of two monoclinic double vanadates, $NaK(VO_3)_2$ and $Na_3K(VO_3)_4$. Glazyrin (1975), however, found only one compound at 50 mole percent KVO_3. The $(Na,K)(V,P)O_3$ system was selected for study to determine whether or not cation substitution on the tetrahedral site results in new structure types. In particular, it was deemed necessary to determine whether there was ordering of V and P, and, if so, whether this ordering resulted in the formation of two inequivalent tetrahedral chains. Furthermore, $NaK(VO_3)_2$ would be expected to adopt the diopside structure with an ordered distribution of Na^+ and K^+ in the M1 and M2 sites, respectively. It was also intended to study the effects of the introduction of a larger cation, K^+, into the $NaVO_3$ lattice on the M1 and M2 sites and the chain configuration. The effects of this type of substitution have been found to lead to changes in the space group symmetry and in the coordination number of M2 in the diopside-enstatite-pigeonite series.

In the present work, three different compounds and solid solutions in the $(Na,K)(V,P)O_3$ system have been synthesized and their crystal structures determined. Site population analysis showed their compositions to be $NaV_{2/3}P_{1/3}O_3$, $Na_{0.5}K_{0.5}VO_3$, and $Na_{.875}K_{.125}VO_3$. All three structures have been refined satisfactorily in the space group C2/c. No violations of the c glide were found.

CHAPTER II

STRUCTURE DETERMINATION BY X-RAY DIFFRACTION

This review of the methods of structure determination will be limited to those methods actually used in the course of the present work.

2.1 Structure Factors

The most important information derived from the measured diffraction intensity is the structure factor modulus or structure factor amplitude, $|F_{hk\ell}|$. If a crystal has mosaic spread, as is generally the case:

$$|F_{hk\ell}| \propto \sqrt{I} \qquad (2.1)$$

The observed structure factors, the F_o's, are derived from the measured intensities by a process of data reduction. The relationship between the observed structure factors and the intensities can also be written:

$$|F_o| = \sqrt{kI/Lp} \qquad (2.2)$$

k is normally a constant for any set of data, and depends on such things as crystal size and beam intensity. k is often omitted and relative structure factors, $|F_{rel}|$, are calculated instead:

$$|F_{rel}| = \sqrt{I/Lp}$$

or

$$k'|F_{rel}| = |F_o| \qquad (2.3)$$

A comparison of the $|F_{rel}|$'s with the $|F_c|$'s, the structure factors calculated on the basis of the model structure, gives the scale factor k' and allows one to determine the $|F_o|$'s. L is the lorentz factor and p is the polarization factor.

2.2 Applied Corrections

2.2.1 The polarization factor, p

The polarization correction must be applied to diffractometer data because of the partial polarization of the X-ray beam by the crystal monochromator and the sample. This polarization is due to the manner in which the reflection efficiency of the X-ray beam varies with 2θ. If the incident X-ray beam is unpolarized, then the electric vector associated with each photon can point in any direction normal to the direction of propagation. Each of these electric vectors can be resolved into two components, one parallel to the reflecting plane, $I_{||}$, and one perpendicular to it, $I_{\perp}$. Half of the beam intensity is associated with $I_{||}$ and half with $I_{\perp}$ because of the random orientation of the electric vectors. The reflection of $I_{||}$ depends only on the electron density in the reflecting plane. However, the reflection of $I_{\perp}$ depends both on the electron density and on $\cos^2 2\theta$. The polarization factor is then:

$$p = 1/2 + 1/2 \cos^2 2\theta \qquad (2.4)$$

For crystal monochromatized radiation the incident beam is already partially polarized before it strikes the sample, and the polarization factor also depends on the Bragg angle for the monochromator, $2\theta_o$. The

polarization correction then becomes:

$$p = \frac{1 + \cos^2 2\theta \cos^2 2\theta_0}{1 + \cos^2 2\theta} \qquad (2.5)$$

2.2.2. The Lorentz factor, L

The time required for a reciprocal lattice point to pass through the sphere of reflection varies both with its position in reciprocal space and with the direction from which it approaches the sphere of reflection. The Lorentz factor, L, is used to correct for this dependence. Consider a reciprocal lattice point r, at a distance d^* from the reciprocal lattice origin, 0. If the crystal and the reciprocal lattice are rotated at a constant angular velocity ω, and r is describing a circle of radius d^* around the origin, then the linear velocity v at which r approaches the sphere of reflection is:

$$v = d^*\omega \qquad (2.6)$$

$$= (2 \sin \theta)\omega$$

The time t required for r to pass through the sphere along a path of length ℓ is:

$$t = \frac{\ell}{v} \qquad (2.7)$$

$$= \frac{\ell}{(2\omega)\sin\theta}$$

ℓ depends on the angle between the surface of the sphere and the path followed by r, and:

$$\ell \propto \frac{1}{\cos\theta} \qquad (2.8)$$

Omitting the constant ω,

$$t \propto \frac{1}{2 \cos \theta \sin \theta} \qquad (2.9)$$

and:

$$2 \cos \theta \sin \theta = \sin 2\theta \qquad (2.10)$$

so:

$$t \propto \frac{1}{\sin 2\theta} \qquad (2.11)$$

The Lorentz factor is related to equation (2.11) by a constant factor:

$$L = \frac{1}{\sin 2\theta} \qquad (2.12)$$

This is not the most general form of the Lorentz factor, but it is applicable in the case of diffractometer data.

2.2.3. Anomalous dispersion

The scattering factor, f_0, is the scattering power of a given atom for a given reflection. It is expressed in terms of the scattering power of an equivalent number of electrons located at the site of the atomic nucleus.

For a point atom f_0 is only a function of atom type. However, for a spherical atom f_0 is a function both of atom type and $\sin \theta/\lambda$. At $\sin \theta/\lambda = 0$, f_0 is equal to the number of electrons in the atom. As $\sin \theta/\lambda$ increases, the scattering from different parts of the atom becomes increasingly out of phase, so that f_0 decreases as $\sin \theta/\lambda$ increases.

The scattering factor must often be corrected for the effects of the phenomenon known as anomalous dispersion or anomalous scattering. If the frequency of the incident beam falls near a natural absorption frequency of one of the scatterers, an anomalous phase change occurs during scattering by the electron associated with the absorption edge. This is anomalous dispersion. The corrected scattering factor, f^{anom}, is a complex number:

$$f^{anom} = f_0 + \Delta f' + i\Delta f'' \qquad (2.13)$$

$$= f' + i\Delta f''$$

2.2.4 Temperature factors

Any increase in the effective size of an atom's electron cloud will result in a more rapid reduction in the scattering factor with increasing $\sin\theta/\lambda$. Thus it is necessary to make some correction for the vibrations of the atoms about their equilibrium positions. The amount of vibration depends on the temperature, atomic mass, and the "stiffness" of the interatomic bonds. The amplitude of vibration increases with temperature. Any increase in the vibration will spread out the electron cloud.

Atomic vibrations are initially assumed to be spherically symmetrical, and the change in scattering power is:

$$T = e^{-B(\sin^2\theta)/\lambda^2} \qquad (2.14)$$

where

$$B = 8\pi^2\overline{u^2} \qquad (2.15)$$

$\overline{u^2}$ is the mean-square amplitude of atomic vibration. Thus for isotropic vibrations

$$f = f_0 e^{-B(\sin^2\theta)/\lambda^2} \qquad (2.16)$$

Later in the refinement the atomic vibrations are assumed to be ellipsoidal rather than spherical. The anisotropic temperature factor is:

$$T = \exp[-2\pi^2(\sum_{i=1}^{3}\sum_{j=1}^{3} U_{ij}h_ih_jb_ib_j)] \qquad (2.17)$$

where the b_i's are reciprocal lattice vectors, the U_{ij}'s are the thermal parameters expressed in terms of mean-square amplitudes of vibration in angstroms, and the h_i's are the Miller indices of the reflection.

2.2.5. Absorption corrections

In general a correction must be made for the absorption of X-rays by the crystal. The intensity of the beam after passing through a region of thickness τ is:

$$I = I_0 e^{-\mu_\lambda \tau} \qquad (2.18)$$

Where I_0 is the intensity of the incident beam and μ_λ is the linear absorption coefficient of the material for a particular type of radiation. Absorption is less of a problem for shorter wavelength radiation, such as Mo, than it is for longer wavelength radiation such as Cu. The absorption coefficient can also be expressed in terms of the density, ρ, of the crystal, and the mass absorption coefficients, $(\mu/\rho)_\lambda$, for the elements present in the crystal.

$$\mu_\lambda = \rho(\mu/\rho)_\lambda \qquad (2.19)$$

If the composition and unit cell parameters of the material are know, then:

$$\mu_\lambda = \rho \sum_n (P_n/100)(\mu/\rho)_{\lambda,E_n} \qquad (2.20)$$

$E_1, E_2, \ldots E_n$ are the elements present in the material and P_n is the weight percent of each element. The mass absorption coefficients are found in the International Tables for X-ray Crystallography (1962).

A transmission factor A is usually defined as:

$$A = \frac{I}{I_o} \qquad (2.21)$$

When the various path lengths in a crystal are unequal, the above expression has to be integrated over the various paths in the volume of the crystal, so:

$$A = \frac{\int^V I dV}{\int^V I_o dV} \qquad (2.22)$$

$$= \frac{\int^V e^{-\mu_\lambda \tau} dV}{V}$$

The transmission factors for crystals with spherical and cylindrical shapes and radius R have been calculated in the form of absorption correction factors A^*, where:

$$A^* = A^{-1} \qquad (2.23)$$

A^* is tabulated as a function of θ and μR in the International Tables for X-ray Crystallography (1959).

2.2.6. Secondary extinction corrections

Absorption of the X-ray beam by the crystal results in a decrease in beam intensity which is independent of θ. However, there is an additional loss of intensity which occurs only when the Bragg reflection conditions are satisfied. In general, there are two possible reasons for this intensity loss, primary and secondary extinction. Only secondary extinction causes significant intensity loss in most cases.

Primary extinction is an interference process involving multiple reflections within the crystal. The effect is small for most imperfect crystals and primary extinction corrections are rarely applied.

Secondary extinction is often encountered in single crystal studies, and the effects are often important, particularly at low $\sin\theta/\lambda$ and for large crystals. Secondary extinction occurs when a reflection is of such intensity that an appreciable amount of the beam is reflected by the first planes encountered, so that the deeper planes reflect less strongly than they should. Crystals with misaligned mosaic blocks have fewer planes in the reflecting position at any one time than do those crystals with well aligned mosaic blocks. Thus secondary extinction effects are less serious for crystals which have badly aligned mosaic blocks. Crystals for which secondary extinction effects are negligible are described as being ideally imperfect. In this work corrections for secondary extinction effects were calculated using the method of Larson (1967). The corrected structure factors are given by the equation:

$$F_c^{corr} = F_c(1 + g\beta F_c^2)^{-1/2} \qquad (2.24)$$

β is a function of both the 2θ angle for the reflection and the Bragg angle of the graphite monochromator (Zachariason, 1963), and g is the secondary extinction parameter incorporated in the least squares refinement.

2.3 Structure Determination and Refinement

2.3.1. Structure Factors and Fourier Series

Assuming that the scattering power of the electron cloud of each atom can be equated with that of the proper number of electrons located at the center of the atom, it is possible to derive an expression for the structure factor, $F_{hk\ell}$, in terms of superposition of waves. If the unit cell contains j atoms, then $F_{hk\ell}$ is the resultant of the j waves scattered in the direction of the reflection hkℓ by the j atoms. The amplitude of each wave is proportional to f_j, the scattering factor for each atom. Each wave has a phase shift, δ, relative to a wave scattered by hypothetical electrons located at the unit cell origin. The phase difference for a wave scattered by an atom at a point (ax, by, cz) is:

$$\delta = 2\pi(hx + ky + \ell z) \qquad (2.25)$$

The magnitude of the structure factor, $|F_{hk\ell}|$, is:

$$|F_{hk\ell}| = (\{\sum_j f_j \cos 2\pi(hx_j + ky_j + \ell z_j)\}^2 + \{\sum_j f_j \sin 2\pi(hx_j + ky_j + \ell z_j)\}^2)^{1/2} \qquad (2.26)$$

$$= \sqrt{A_{hk\ell}^2 + B_{hk\ell}^2}$$

where

$$A_{hk\ell} = \sum_j f_j \cos 2\pi(hx_j + ky_j + \ell z_j) \qquad (2.27)$$

$$B_{hk\ell} = \sum_j f_j \sin 2\pi(hx_j + ky_j + \ell z_j)$$

The phase of the resultant $F_{hk\ell}$ is:

$$\alpha_{hk\ell} = \arctan \frac{B_{hk\ell}}{A_{hk\ell}} \qquad (2.28)$$

Since the structure factor can be represented as a wave, it can reasonably be expressed as a complex number in rectangular form:

$$F_{hk\ell} = A_{hk\ell} + iB_{hk\ell} \qquad (2.29)$$

$$= \sum_j f_j e^{2\pi i(hx_j + ky_j + \ell z_j)}$$

The structure factor can also be thought of as the sum of wavelets scattered by the elements of electron density, $\rho(x,y,z)$, in the unit cell, without considering the nature of the distribution of the electron density.

$$F_{hk\ell} = \int_V \rho(x,y,z) e^{2\pi i(hx + ky + \ell z)} dV \qquad (2.30)$$

During structure refinements it is often necessary to calculate electron distributions based on a set of structure factors. Since crystals are periodic structures, they can be represented by periodic functions such as Fourier series. The electron density, $\rho(x,y,z)$, can be represented by a three dimensional Fourier series as follows:

$$\rho(x,y,z) = \sum_{h'} \sum_{k'} \sum_{\ell'} C_{h'k'\ell'} e^{2\pi i(h'x + k'y + \ell'z)} \qquad (2.31)$$

where h', k', ℓ' are integers between $-\infty$ and ∞. Substituting equation 2.31 into equation 2.30 gives:

$$F_{hk\ell} = \int_V \sum_{h'} \sum_{k'} \sum_{\ell'} C_{h'k'\ell'} e^{2\pi i(h'x + k'y + \ell'z)} \qquad (2.32)$$

$$\times\ e^{2\pi i(hx + ky + \ell z)} dV$$

$$= \int \sum_{h'} \sum_{k'} \sum_{\ell'} C_{h'k'\ell'} e^{2\pi i[(h + h')x + (k + k')y + (\ell + \ell')z]} dV$$

This integral vanishes unless

$$h' = -h \qquad (2.33)$$

$$k' = -k$$

$$\ell' = -\ell$$

Then:

$$F_{hk\ell} = \int_V C_{\bar{h}\bar{k}\bar{\ell}}\, dv = V\, C_{\bar{h}\bar{k}\bar{\ell}} \qquad (2.34)$$

and

$$C_{\bar{h}\bar{k}\bar{\ell}} = \frac{1}{V} F_{hk\ell} \qquad (2.35)$$

In other words, the structure factors are proportional to the Fourier coefficients of the three-dimensional Fourier series, equation 2.31 and:

$$\rho(x,y,z) = \frac{1}{V} \sum_{h} \sum_{k} \sum_{\ell} F_{hk\ell} e^{2\pi i(hx + ky + \ell z)} \qquad (2.36)$$

The electron density is said to be the Fourier transform of the structure factors, and vice versa.

Several different types of Fourier series are used in crystallographic studies. The results depend on the type of coefficients used. The electron density can be calculated using equation 2.36. The moduli of the structure factors, $|F_{hk\ell}|$ or $|F_o|$ can be found from the intensity data, as has been previously described. Unfortunately, the $F_{hk\ell}$ in equation 2.36 are not the phaseless moduli, so that phases must be determined somehow.

Once a preliminary model has been chosen, it can be used to calculate a set of F_c, complete with phases. These phases can be used, with the values of $|F_o|$ obtained from the intensity data, to calculate an electron density map.

2.3.2. The Patterson Function

One of the most important ways of deriving model structures is through the use of the Patterson or $|F|^2$ function. A.L. Patterson (1935) showed that the $|F_o|^2$'s can be used as coefficients of a Fourier series whose peaks represent, not atomic positions, but the terminal points of interatomic vectors drawn from the origin. Thus there is a large peak at the origin which represents the zero vectors resulting from the interaction of each atom with itself. The Patterson function has the property that its space group is the same as that of the crystal, with the addition, if necessary, of a center of symmetry. The interpretation of the Patterson function involves the determination of the positions of all of the atoms relative to some fixed origin. The Patterson function has the form:

$$P(u,v,w) = \frac{1}{V} \sum_h \sum_k \sum_\ell |F_{hk\ell}|^2 \cos 2\pi(hu + kv + \ell w) \qquad (2.37)$$

2.3.3. The Difference Synthesis

The last Fourier synthesis which will be considered here is the difference synthesis or difference Fourier. The Fourier coefficients are the ΔF's, $|F_o| - |F_c|$. The phases derived from the model structure are used with both the F_o's and the F_c's. Thus the difference synthesis consists of an F_o synthesis, calculated using the phases due to the model, minus an F_c synthesis calculated with F_c phases and F_c moduli. This type of synthesis is very useful for locating new atoms and correcting the positions of those present in the model. The difference synthesis is calculated as follows:

$$\Delta\rho(x,y,z) = \frac{1}{V} \sum_h \sum_k \sum_\ell \Delta F e^{-2\pi i(hx + ky + \ell z)} \qquad (2.38)$$

2.3.4. Least squares refinement

Given some reasonably correct model structure, it is possible to refine atomic, thermal, and scale parameters using the method of least squares. The percent occupancy of a site by different atoms can also be determined.

Consider the function $|F|$, whose value is determined by the Miller indices, H, for each reflection, where $H = (h,k,\ell)$, and by the n independent parameters $p_1, p_2, \ldots p_n$ which define the function. The p_i's include the atomic positions, temperature factors, scale factors, and site occupancy. The Miller indices are known as "location" variables. The value of $|F|$

can be measured at each of the N different Bragg peaks, where $N > n$. The principle of least squares states that the best values for $p_1, \ldots p_n$ are those which minimize the sum of the squares of the weighted differences between the F_o's and the F_c's for all reflections. Thus one wishes to minimize the function:

$$D = \sum_H w(H)[|F_o(H)| - |F_c(H)|]^2 \qquad (2.39)$$

$w(H)$ is the weight assigned to each reflection. Minimizing D implies that $\frac{\partial D}{\partial p_i} = 0$ for each p_i.

Thus:

$$\sum_H w(H)[|F_o(H)| - |F_c(H)|]\frac{\partial |F_c(H)|}{\partial p_i} = 0 \qquad (2.40)$$

$$(i = 1,2, \ldots n)$$

$|F_c|$ is a transcendental function and can be expanded as a Taylor series. If $p = (p_1, p_2, \ldots p_n)$ represents the "true" value for independent parameters, and $q = (q_1, q_2 \ldots q_n)$ is close to p, then $\delta_i = p_i - q_i$ is small for all i. Expanding to first order only gives:

$$|F_c(H;p)| = |F_c(H;q)| + \sum_{i=1}^{n} \frac{\partial |F_c(H;q)|}{\partial p_i}\delta_i \qquad (2.41)$$

Now the function is linear in δ_i with coefficients $\frac{\partial |F_c(H;q)|}{\partial p_i}$

Substituting equation 2.41 into equation 2.40 and simplifying results in a system of n equations of the form:

$$\sum_{j=1}^{n} \sum_{H} w(H)\left(\partial|F_c(H;q)|/\partial p_i\right)\left(\partial|F_c(H;q)|/\partial p_j\right)\delta_j$$

$$= \sum_{H} w(H)[|F_o(H)| - |F_c(H;q)|]\partial|F_c(H;q)|/\delta p_i$$

$$(i = 1, 2, \ldots n) \qquad (2.42)$$

This set of n equations in n unknowns, the δ_j's, is the set of normal equations. The normal equations are linear and solvable in the δ_j's. Starting the refinement with the approximate parameters q will give a better, but still approximate set of parameters at the end of the first cycle of refinement. The process can be repeated until there is convergence, and further refinement leads to no significant change in the parameters.

2.3.5. Weighting functions

When using the method of least squares it is necessary to assign a weight to each reflection based on the precision of measurement. A good weighting scheme adjusts the contribution of each reflection to the normal equations so as to produce the most reliable results. The weighting scheme used has the form:

$$w = [A + B\,(k|F_o|) + C(k|F_o|)^2 + D(\sigma[F_o]/|F_o|)^2]^{-1} \qquad (2.43)$$

where A, B, C and D are weighting coefficients and k is the scale factor relating F_o and F_c. The coefficients are adjusted so that the square of the difference between the observed and calculated structure factors, $||F_o|-|F_o||^2$, is independent of F_o.

Initially, those reflections with $I < 3\sigma(I)$ are considered to be unobserved and are excluded from the refinement. In the last stages of refinement they are flagged as observed and included in the calculations. The justification for this is that the $3\sigma(I)$ cut-off is arbitrary, and that the results are less biased by the use of a good weighting scheme, which will minimize the contributions of the weak reflections, than by their exclusion from the refinement. It has been observed, however, that including the unobserved reflections produces a slight increase in R.

2.3.6. The residual index, R

The residual index, R, is defined as:

$$R = \frac{\sum ||F_o| - |F_c||}{\sum |F_o|} \qquad (2.44)$$

and is a measure of the agreement between the actual structure and the model used. The theoretical R values for a model containing the correct number and kind of atoms arranged randomly have been determined (Wilson, 1950).

$$R \text{ random, centric} = 0.83 \qquad (2.45)$$

$$R \text{ random, acentric} = 0.59$$

In general, acentric structures will have lower R values than centric structures at the same stage of refinement.

It is possible to calculate an R value as low as 0.2 to 0.3 on the basis of an incorrect model. In general, however, a structure which refines to an R value in this range within a couple of cycles is probably a good approximation to the true structure. All the present structures

are centric, with space group C2/c. .The R values at the end of the final cycle of refinement were all below 0.08, showing good agreement between the observed and calculated structures.

The weighted residual index, R_w, is defined as:

$$R_w = \left(\frac{\sum w(|F_o| - |F_c|)^2}{\sum w |F_o|^2} \right)^{1/2} \qquad (2.46)$$

It is calculated along with R and can be used to estimate the effectiveness of the weighting scheme.

2.3.7 Site Occupancy and Composition

In each of the current structure determinations it was necessary to calculate the percentage occupancy of one site by two atom types. This problem is dealt with in different ways by different refinement programs. Given the possible atom types and the total site occupancy, the program RFINE (Finger, 1969) will determine the amount of one element present and adjust the amount of the other element accordingly. The CUDLS full-matrix least squares program (Stephens, 1974) can also be used to determine the occupancy of a site by two different chemical species. Given a reasonable idea of the composition of a crystal, based on the composition of the reaction mixture, a previously determined phase diagram, or analytical data, it is possible to calculate a composite scattering curve. For instance, if a crystal is grown from a reaction mixture with a% A and (100-a)% B, then the composite scattering factor is given by:

$$f_c = \frac{(af_A + (100-a)f_B)}{100} \qquad (2.47)$$

for each value of sin θ/λ. While such a mixed scattering curve may be useful during the preliminary stages of refinement, its usefulness depends upon the reliability of the information on which it is based. In a situation where two species share a common site, good analytical data will completely determine the problem. However, if two species can occupy two sites, then even the best analysis will not determine the occupancy of individual sites. A quite satisfactory way of determining site occupancy and overall composition is to assume that a given site is occupied exclusively by one type of atom. If the site multiplicity shows a significant change on refinement, then it is possible to estimate the percent occupancy of the site by the two species. For example, if V, with 23 electrons, and P, with 15 electrons, both occupy a site which is found to contain the equivalent of 0.80 V, then x, the fraction of V present, is found as follows:

$$0.80 \times 23 = 23x + 15\,(1-x) \qquad (2.48)$$

Here x is 0.425, so the site occupancy is 42.5% V and 57.5% P.

The positional and thermal parameters are refined for only one of the atoms, and only half of the calculated correction is applied to avoid overcompensating. The positional and thermal parameters of the second atom are adjusted before the next cycle of refinement.

2.4. Computer Programs

2.4.1. The X-ray 71 System

The X-ray 71 system (1971) is a collection of related Fortran programs designed for use in all aspects of crystal structure determination,

from setting the diffractometer and initial data reduction to calculation of Fourier syntheses, least squares refinements, and direct methods of phase determination. The X-ray '71 programs which have been used in this work are:

1. DATCO3 - DATCO3 is used in the preprocessing of diffractometer data. It sorts the data, averages equivalent reflections, and flags reflections as "less-thans" according to specified criteria. The sorted, averaged data may be punched on cards, or placed in a file in preparation for data reduction.

2. DATRDN - DATRDN can be used for processing raw intensity data. It calculates $\sqrt{I}$ and applies the Lp corrections appropriate to the method of data collection. There are provisions for applying absorption and anomalous dispersion corrections.

3. DUMCOP - DUMCOP will dump, copy, or punch on cards the contents of a binary data file. It is normally used to produce card output for use by one of the Fourier synthesis or least squares refinement programs. It can also be used to examine a binary data file.

Fourier syntheses, of the ΔF, F_o, and Patterson types can be produced by using the program sequence. DATRDN, LOADAT, FC and FOURR.

4. LOADAT - LOADAT loads atom parameters in the binary data file. It must be used before any program which calculates structure factors, FC, for example.

5. FC - FC reads the atomic parameters from the binary data file and generates the complete unit cell contents. It then calculates the structure factors.

6. FOURR - FOURR calculates several types of Fourier series including F_o, F_c, difference and Patterson syntheses, and E maps, and prints them as maps suitable for contouring.

The combination of DATRDN and NORMSF can be used to calculate normalized structure factors for use in direct methods. The expected normalized structure factors are calculated for centric and acentric models and compared with the actual values to determine whether or not the structure has a centre of symmetry.

7. NORMSF - NORMSF calculates the quasi-normalized structure factors, E. Four methods are used to estimate scale and thermal parameters, resulting in four values of E.

8. PARAM - PARAM is used in the least squares refinement of unit cell parameters using two-theta data.

2.4.2. CUDLS

CUDLS calculates structure factors and refines the independent parameters of a model structure by full-matrix least squares methods. The program was written by J.S. Stephens of McMaster University (1974). It will accept up to 44 atoms per asymmetric unit, ten species, sixteen scale factors and it will do up to five cycles of refinement. Isotropic and anisotropic temperature factors are given as U_j's or U_{ij}'s respectively. The U's are the mean square amplitudes of vibration in $\AA^2$. The program is capable of refining the scale factors, positional and thermal parameters of the atoms, site multiplicity and a parameter used to correct for secondary extinction. It will also calculate bond angles and distances for up to fifteen neighbouring atoms.

2.4.3. RFINE

RFINE (Finger, 1969) is a full matrix least squares refinement program written by L.W. Finger. It is very useful in dealing with structures where disorder or multiple site occupancy is suspected. The program will accept up to sixty atoms, twenty chemical species, ten scale factors, two hundred parameters and forty parameter dependencies. Any combination of isotropic or anisotropic thermal parameters is allowed.

The program can handle constraints of positional and thermal parameters for atoms in special positions. Given the total occupancy of a site and the species present, the program will refine the percentage of each species present. In the case of a disordered structure where several positions may be occupied by one species, the chemical composition may also be constrained.

CHAPTER III

THE CRYSTAL STRUCTURE OF $Zn_3V_{0.5}P_{1.5}O_8$

3.1. Results

3.1.1. Experimental

A reaction mixture containing 56 mole percent $Zn_3(VO_4)_2$ and 44 mole percent $Zn_3(PO_4)_2$ was finely ground and calcined in a Pt crucible at 600^oC for one day. It was then quenched in air, reground, and held at 1000^oC for one day. The melt was then cooled rapidly to 900^oC, cooled at a rate of 3^oC/hr to about 775^oC and quenched to room temperature. A colourless crystal with dimensions 0.10 x 0.08 x 0.04 mm was chosen for intensity measurements. Accurate unit cell parameters were obtained by refining the 2θ values of 15 reflections having 2θ values falling between 25 and 30^o.

Intensity data were measured on a Syntex $P\bar{1}$ four-circle automatic diffractometer using graphite monochromatized MoKα radiation and a θ/2θ scan mode. In the θ/2θ technique the crystal is rotated to carry the reciprocal lattice point from the outside of the sphere of reflection to the inside, while the counter rotates at twice the angular frequency of the crystal. Thus it is possible to scan along the line connecting the lattice point with the reciprocal lattice origin. The θ/2θ scan mode is used because it enables one to scan over white radiation streaks as well as over the Bragg peak, so that one can measure the background. The background is scanned before and after scanning each Bragg peak.

A total of 910 symmetry independent reflections with $I>0$ were collected within a sphere defined by $2\theta<60°$. Absorption corrections were applied assuming the crystal to be a sphere of radius 0.04 mm ($\mu R = 0.49$).

3.1.2. Crystal Data at 21°C

$Zn_3V_{0.5}P_{1.5}O_8$ F.W. = 396.04

Monoclinic

$a = 15.941(6)$ Å $b = 5.314(2)$ Å $c = 8.265(2)$ Å

$\beta = 106.96(3)°$

$V = 669.59$ Å^3

$Z = 4$

$D_x = 3.92$ g/cm^3

Space group = C2/c

Systematic absences: $h+k$ odd, in general

$h0\ell$ ℓ odd

The structure was derived from the Patterson function. The final discrepancy factors were:

$R = 0.073$

$R_w = 0.056$

The final weighting scheme was:

$$w = [10.7 + 0.073\ k|F_o| + 0.0005\ (k|F_o|)^2 + 3500(\sigma[F_o]/|F_o|)^2]^{-1} \quad (3.1)$$

The refined secondary extinction parameter was $4.1(7) \times 10^{-6}$. The final position and thermal parameters are listed in Tables 3.1a and 3.1b respectively.

TABLE 3.1a

Positional parameters for $Zn_3V_{0.5}P_{1.5}O_8$ with estimated standard deviations in parentheses

Atom	x	y	z
Zn(1)	0	0.0587(3)	3/4
Zn(2)	0.18558(6)	0.7929(2)	0.7137(1)
X*	0.1209(3)	0.292(1)	0.5294(6)
O(1)	0.6021(4)	0.672(1)	0.3456(8)
O(2)	0.6491(4)	0.931(1)	0.0253(7)
O(3)	0.4601(4)	0.747(1)	0.9089(8)
O(4)	0.2964(4)	0.638(1)	0.8495(7)

*X = 0.25(2)V + 0.75P

TABLE 3.1b

Thermal parameters** for $Zn_3V_{0.5}P_{1.5}O_8$ with estimated standard deviations in parentheses

Atom	U_{11}	U_{22}	U_{33}	U_{12}	U_{13}	U_{23}
Zn(1)	13.1(6)	14.7(6)	19.0(7)	-	6.5(5)	-
Zn(2)	16.3(4)	98(4)	18.2(5)	2.1(4)	5.5(3)	0.7(4)
X*	11(2)	10(2)	11(2)	-2(2)	3(2)	-1(2)
O(1)	20(3)	19(3)	21(3)	-5(2)	8(2)	-2(2)
O(2)	21(3)	16(3)	16(3)	5(2)	3(2)	2(2)
O(3)	16(3)	25(3)	19(3)	-2(2)	6(2)	-1(2)
O(4)	16(3)	9(2)	14(3)	2(2)	1(2)	-3(2)

*X = 0.25(2)V + 0.75P

**The temperature factor expression is $\exp[-2\pi^2 \times 10^{-4}(U_{11}h^2b_1^2+\ldots 2U_{12}hkb_1b_2+\ldots)]$ where the b_i's are reciprocal lattice vectors.

3.1.3. Description of the Structure

Although the structure of $Zn_3V_{0.5}P_{1.5}O_8$ differs from those of both its end members, it most resembles that of α-$Zn_3(PO_4)_2$. α-$Zn_3(PO_4)_2$ is monoclinic, with space group C2/c and a = 8.196, b = 5.634, c = 15.007 Å, β = 105.0°, and Z = 4 (Calvo, 1965, and Calvo and Faggiani, unpublished results). All the cations are tetrahedrally coordinated. α-$Zn_3(VO_4)_2$, on the other hand, is orthorhombic with space group Cmca and a = 6.088, b = 11.489, c = 8.280 Å (Gopal and Calvo, 1971). The Zn ions are found in two types of octahedral sites and the V^{5+} is tetrahedrally coordinated.

In the present structure, as in α-$Zn_3(PO_4)_2$, all the cations are tetrahedrally coordinated (Figure 3.1). The $Zn(1)O_4$ and XO_4 tetrahedra (X = V,P) are linked, each at two corners, to form four-membered rings about the centers of symmetry. These rings form chains parallel to the c axis, which are generated by the two-fold axis through Zn(1) and the action of the centers of symmetry. Adjacent chains are joined by Zn(2) tetrahedra. The $Zn(2)O_4$ groups form chains parallel to the b axis. O(4) is the bridging oxygen. Adjacent tetrahedra are related by the two-fold screw axis. Each oxygen in the $Zn(2)O_4$ tetrahedron is shared with a different XO_4 group.

The average X-O bond length is 1.575 Å. If Vegard's law holds, then the composition weighted average of the <P-O> (1.537 Å) and <V-O> (1.721 Å) (Gopal, 1972) for tetrahedral coordination should be 1.583 Å.

The X-O bond lengths reflect the environments of the oxygen atoms (Table 3.2). The shortest X-O bonds are those to O(2) and O(3).

Figure 3.1 The Structure of $Zn_3V_{0.5}P_{1.5}O_8$

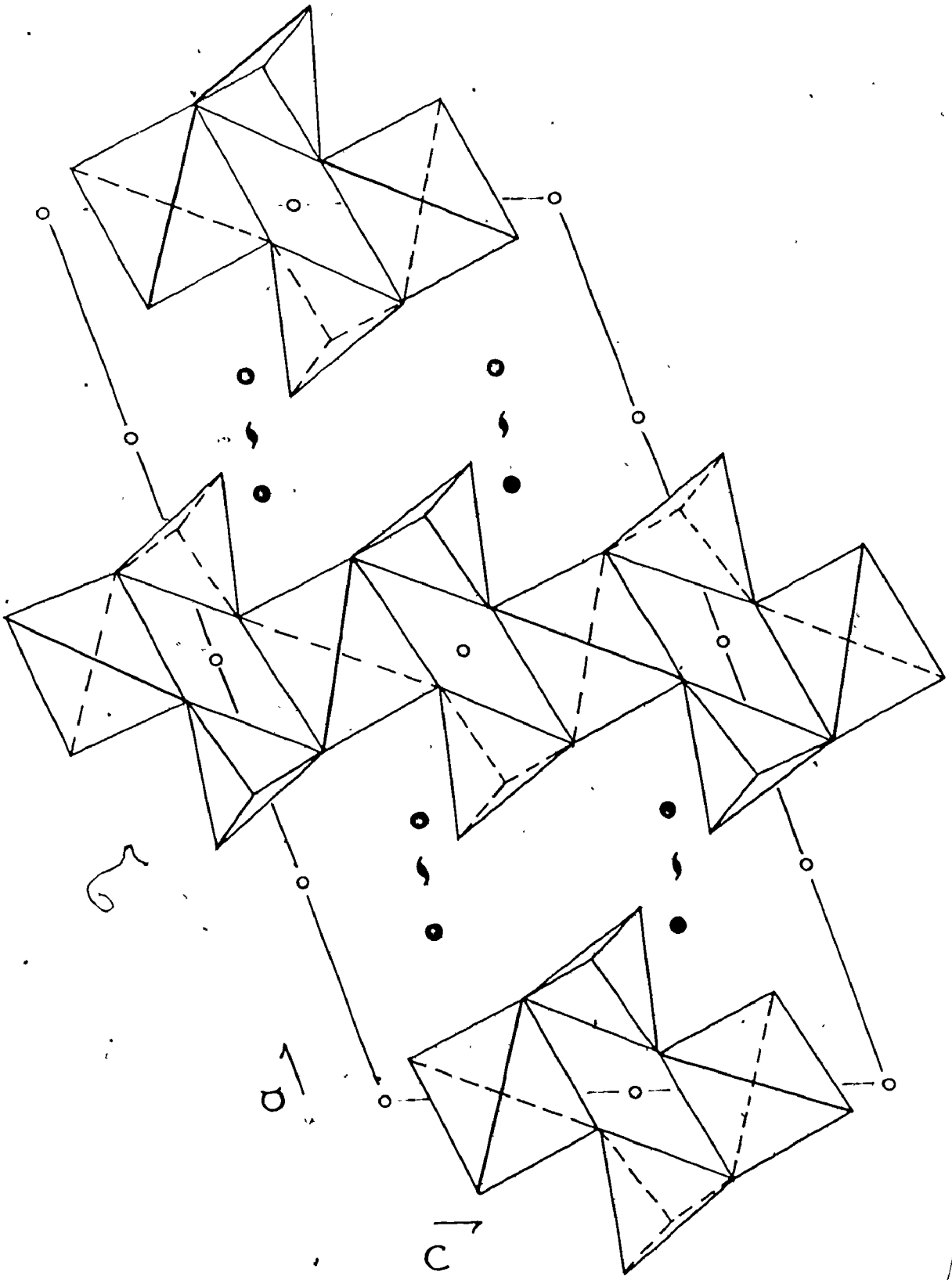
c
a
C

TABLE 3.2

Bond Lengths and Bond Angles in

$Zn_3V_{0.5}P_{1.5}O_8$

Bond	Distance (Å)		Bonds	Angle (deg)
Zn(1)-O(1)	2.007(6)	2x	O(1)-X-O(2)	109.6(5)
-O(3)	1.902(7)	2x	-O(3)	108.1(4)
			-O(4)	106.2(4)
Zn(2)-O(1)	1.960(7)			
-O(2)	1.911(6)		O(1)-Zn(1)-O(3)'	101.4(3)
-O(4)	1.976(5)			
-O(4)'	1.948(6)		O(3)-Zn(1)-O(3)'	116.6(3)
			O(2)-Zn(2)-O(4)	102.2(2)
X-O(1)	1.593(8)		-O(4)'	113.6(2)
-O(2)	1.541(8)			
-O(3)	1.539(9)		O(4)-Zn(2)-O(4)'	111.6(2)
-O(4)	1.626(5)			
			O(2)-X-O(3)	115.7(5)
Bonds	Angle (deg)		-O(4)	107.8(4)
O(1)-Zn(1)-O(1)'	104.6(3)		O(3)-X-O(4)	108.9(5)
-O(3)	116.5(3)			
O(1)-Zn(2)-O(2)	114.7(3)			
-O(4)	111.3(3)			
-O(4)'	103.7(3)			

Both O(2) and O(3) are shared by X and only one Zn. O(1) and O(4) are each shared by X and two Zn ions. The average Zn O(1) bond is longer (1.934 Å) than the average Zn O(4) bond (1.962 Å) and as a result the X O(4) bond (1.626 Å) is longer than the X O(1) bond (1.593 Å). The average Zn O(2), Zn O(3) and X-O(2) and X O(3) bond distances are not significantly different. The major angular distortion of the XO_4 group involves a large O(2) X O(3) bond angle, reflecting an enhanced repulsion between the two oxygens because of the short X O bond lengths.

Both ZnO_4 groups show a large range of O-Zn-O' angles, although the $Zn(2)O_4$ group is more regular. The Zn(1) atoms are displaced towards the O(3) - O(3)' edge. The O(n)-Zn(1)-O(n)' angle is 116.6° for n=3 and 104.6° for n=1. The O(3) - O(3)' and O(1) - O(1)' edges are twisted about the two-fold axis so as to subtend an angle deviating by 10° from the orthogonality required for a regular tetrahedron.

The range of bond lengths and bond angles is smaller for the $Zn(2)O_4$ group than for the $Zn(1)O_4$ group. The mean Zn(n)-O bond lengths are 1.955 Å for n=1 and 1.948 Å for n=2. These differences are hardly significant, although Zn(1) has six neighbouring cations and Zn(2) has only five.

3.2. Discussion

Previously, α-$Zn_3(PO_4)_2$ was thought to be the only compound with $M_3X_2O_8$ stoichiometry in which all the cations displayed tetrahedral coordination (Calvo, 1965). In β-$Zn_3(PO_4)_2$ (Stephens and Calvo, 1967)

there are three independent Zn sites and two independent P sites. Zn(1) is bonded to four oxygens to form an irregular tetrahedron. Zn(2) and Zn(3) are both bonded to five oxygens. P(1) and P(2) are both roughly tetrahedral. In γ-$Zn_3(PO_4)_2$, which is really a solid solution $(M',M'')_3(PO_4)_2$, where M' Zn and M" can be Mn^{2+}, Mg^{2+}, Ca^{2+} or Cd^{2+} (Calvo, 1968a) the PO_4 groups are approximately tetrahedral and the M cations adopt five and six-fold coordination, with the added cations preferring the octahedral site (Calvo, 1963).

In both α-$Zn_3(PO_4)_2$ and $Zn_3V_{0.5}P_{1.5}O_8$ the Zn(1) lie on the two-fold axes. In α-$Zn_3(PO_4)_2$ the $Zn(1)O_4$ and PO_4 groups form spirals running along b, with a pitch equal to b. The spiral axis coincides with the two-fold screw axis. These spirals form sheets parallel to a. The c glide plane relates groups in adjacent sheets. In the present structure the c glide plane relates groups within the same sheet. The $Zn(2)O_4$ group lie in general positions in both structures, and serve to join adjacent $Zn(1)O_4$-PO_4 (or XO_4) sheets. However, in α-$Zn_3(PO_4)_2$, adjacent groups edge-share across centers of symmetry, while in $Zn_3V_{0.5}P_{1.5}O_8$ they form spiral chains generated by the two-fold screw axes.

The <Zn-O> distance is 1.956 Å in α-$Zn_3(PO_4)_2$ and 1.950 Å in $Zn_3V_{0.5}P_{1.5}O_8$. The discrepancy falls within the uncertainty limits on the bond distances, so no significance can be attached to it.

The XO_4 tetrahedra in $Zn_3V_{0.5}P_{1.5}O_8$ and α-$Zn_3(PO_4)_2$ show similar angular distortions from ideality. The angle subtended at the X atom by those oxygens bonded to only one Zn and one X is 115.4(3)°

in α-$Zn_3(PO_4)_2$ and 115.7(5)° in the present structure. In α-$Zn_3(PO_4)_2$ the O(1)-Zn(1)-O(1)' angle is 102°, where O(1) is three-fold coordinated. O(4) is two-fold coordinated and the O(4)-Zn-O(4)' angle is 130°. In $Zn_3V_{0.5}P_{1.5}O_8$, O(1) is three-fold coordinated and the O(1)-Zn(1)-O(1)' angle is 104.6(3)°. The two-fold coordinated oxygen is O(3) and the O(3)-Zn(1)-O(3)' angle is 116.6(3)°.

It appears that V and P are distributed at random throughout the present structure. Precession photographs showed no signs of long-range ordering and the thermal parameters are not abnormally large.

The question of why $Zn_3V_{0.5}P_{1.5}O_8$ adopts the present structure instead of that of α-$Zn_3(PO_4)_2$ may be at least partially answered by considering Pauling's rules concerning the nature of cation coordination polyhedra (Pauling, 1961). Edge-sharing between the coordination polyhedra of small, highly charged cations should decrease the stability of the structure according to Pauling's third rule. In the α-$Zn_3(PO_4)_2$ structure the Zn(2) tetrahedra share edges, while in $Zn_3V_{0.5}P_{1.5}O_8$ there is no edge-sharing between tetrahedra. This absence of edge-sharing should balance the tendency of cation substitution to destabilize the structure.

CHAPTER IV

THE CRYSTAL STRUCTURES OF THREE MEMBERS OF THE $(Na,K)(V,P)O_3$ SYSTEM

4.1. Results

4.1.1. Experimental

a) $NaV_{2/3}P_{1/3}O_3$ - A mixture with a 2:1:1 molar ratio of $NaPO_3$, V_2O_5, and $Na_2CO_3 \cdot H_2O$ was heated to 900°C in a Pt crucible and cooled slowly to about 500°C. A clear, colourless, needle-like crystal with dimensions 0.10 x 0.15 x 0.30 mm was used to collect intensity data. Intensities were collected on a Syntex $P\bar{1}$ automatic diffractometer as has been previously described (Section 3.1.1). Accurate cell parameters were found by centering 15 reflections with 2θ values lying between 20 and 40°. 604 symmetry independent reflections with $I > 0$ were collected within a sphere defined by $2\theta \leq 55°$. Absorption corrections were applied assuming a cylindrical crystal shape ($\mu R = 0.58$).

b) $Na_{0.5}K_{0.5}VO_3$ - A melt containing approximately 50 mole percent KVO_3 and 50 mole percent $NaVO_3$ was cooled slowly from 560°C to 460°C in a Pt crucible as suggested by the phase diagram (Perraud, 1974). A clear, colourless, fibrous crystal with dimensions 0.06 x 0.06 x 0.35 mm was used to determine the unit cell parameters and diffraction intensities. The accurate unit cell parameters were found by centering 15 reflections with 2θ between 20° and 40°. 772 reflections with $I > 0$

were collected within a sphere defined by $2\theta \leq 55°$. Absorption corrections were made assuming a cylindrical crystal shape ($\mu R = 0.33$).

c) $Na_{.875}K_{.125}VO_3$ - A mixture of V_2O_5, $Na_2CO_3 \cdot H_2O$, and K_2CO_3 with a mole ratio of 4:3:1 was heated to about 600°C in a Pt crucible, held at 549-552°C for a couple of days, and then quenched in air. A clear, colourless, needle-like crystal with dimensions 0.32 x 0.13 x 0.11 mm was used to collect intensity data and determine unit cell parameters. Intensity data were collected using a Syntex $P2_1$ four-circle automatic diffractometer, using graphite monochromatized MoKα radiation and a $\theta/2\theta$ scan mode. The accurate unit cell parameters were found by centering 15 reflections with 2θ between 23° and 41°. 505 symmetry independent reflections with $I > 0$ were collected within a sphere defined by $2\theta \leq 55°$.

The crystal used in data collection was later found to be twinned. The twin components were related by a two-fold rotation around a^*. The intensity data used were those of the major twin component, which was found to have a volume 4.7 times that of the minor twin component. Only the hk0 reflections were superposed by this twinning. The F_o's for these reflections were reduced by a factor of $\sqrt{\frac{4.7}{5.7}}$ before being used in the refinement. One reflection was excluded from the refinement as the result of a probable accidental superposition.

4.1.2. Crystal data at 21°C

a) $NaV_{2/3}P_{1/3}O_3$

Monoclinic F.W. = 115.27

a = 10.421(1) Å

b = 9.475(1) Å

c = 5.715(1) Å

β = 107.62(1)°

V = 537.83 $Å^3$

Z = 8

Dx = 2.85 g/cm^3

Space group: C2/c

Systematic absences: h+k odd, in general

h0ℓ ℓ odd

The positions of the cations were derived from the Patterson function, and the positions of the oxygens were based on those in $NaVO_3$ as determined by Marumo et al. (1974). The final discrepancy factors were:

$$R = 0.035$$

$$R_w = 0.032$$

Weights were set equal to:

$$w = [1.0 + 0.010k|F_o| + 0.00008(k|F_o|)^2 + 300(\sigma[F_o]/|F_o|)^2]^{-1} \quad (4.1)$$

The final positional parameters are listed in Table 4.1a. The thermal parameters are listed in Table 4.1b.

TABLE 4.1a

Positional parameters for $NaV_{2/3}P_{1/3}O_3$
with standard deviations in parentheses

ATOM	x	y	z
X*	.29158(5)	.08864(5)	.25990(9)
M1†	0	.9086(2)	1/4
M2††	0	.2918(2)	1/4
O1	.1299(2)	.0982(2)	.1690(4)
O2	.3561(2)	.2416(2)	.3226(4)
O3	.3510(2)	.0087(3)	.0336(5)

* X = .658(4)V + .342P

† M1 = Na

†† M2 = Na

TABLE 4.1b

**Thermal parameters for $NaV_{2/3}P_{1/3}O_3$ with standard deviations in parentheses

ATOM	U(1,1)	U(2,2)	U(3,3)	U(1,2)	U(1,3)	U(2,3)
X*	.0112(3)	.0141(3)	.0129(3)	-.0016(2)	.0022(2)	-.0010(2)
M1†	.0235(9)	.0230(9)	.0218(8)	0	.0045(6)	0
M2††	.044(1)	.028(1)	.033(1)	0	-.0063(9)	0
O1	.021(1)	.026(1)	.019(1)	-.0029(9)	.0032(8)	-.0001(8)
O2	.031(1)	.030(1)	.029(1)	-.011(1)	.009(1)	-.0024(9)
O3	.022(1)	.035(1)	.042(1)	-.001(1)	.007(1)	-.011(1)

† M1 = Na

†† M2 = Na

* X = .658(4)V + .342P

** The expression for the temperature factor is $\exp[-2\pi^2(\sum_{i=1}^{3}\sum_{j=1}^{3} U_{ij} h_i h_j b_i b_j)]$ where the b_i's are reciprocal lattice vectors.

b) $Na_{0.5}K_{0.5}VO_3$

Monoclinic F.W. = 129.98

a = 10.533(1) Å

b = 9.997(1) Å

c = 5.804(2) Å

β = 104.17(1)°

V = 592.56 $Å^3$

Z = 8

Dx = 2.92 g/cm^3

Space group: C2/c

Systematic absences: h+k odd, in general

h0ℓ ℓ odd

$NaV_{2/3}P_{1/3}O_3$ positional parameters were used to initiate the refinement. The final discrepancy factors were:

$$R = 0.049$$

$$R_w = 0.042$$

and weights were set equal to:

$$w = [2.0 + 0.02k|F_o| + 0.00005(k|F_o|)^2 + 600(\sigma[F_o]/|F_o|)^2)]^{-1} \qquad (4.2)$$

The refined secondary extinction parameter was $6(5) \times 10^{-8}$. The final positional and thermal parameters are listed in Tables 4.2a and 4.2b respectively.

TABLE 4.2a

Positional parameters for $Na_{0.5}K_{0.5}VO_3$ with standard deviations in parentheses

ATOM	x	y	z
V	.28614(6)	.08586(7)	.2240(1)
M1†	0	.9048(2)	1/4
M2††	0	.3077(1)	1/4
O1	.1254(3)	.0888(3)	.1524(5)
O2	.3441(3)	.2364(3)	.2874(5)
O3	.3471(3)	.0153(3)	-.0141(5)

† M1 = Na

†† M2 = K

TABLE 4.2b

** Thermal parameters for $Na_{0.5}K_{0.5}VO_3$ with standard deviations in parentheses

ATOM	U(1,1)	U(2,2)	U(3,3)	U(1,2)	U(1,3)	U(2,3)
V	.0119(3)	.0154(3)	.0091(3)	-.0009(3)	.0020(2)	-.0002(3)
M1 †	.019(1)	.019(1)	.018(1)	0	.0025(9)	0
M2 ††	.0311(8)	.0193(6)	.0203(6)	0	-.0036(5)	0
O1	.015(1)	.026(2)	.018(1)	.002(1)	.003(1)	.002(1)
O2	.034(2)	.019(1)	.023(2)	-.009(1)	.005(1)	-.001(1)
O3	.017(1)	.027(2)	.013(1)	.001(1)	.004(1)	-.004(1)

† M1 = Na

†† M2 = K

** The expression for the temperature factor is $\exp[-2\pi^2(\sum_{i=1}^{3}\sum_{j=1}^{3} U_{ij}h_ih_jb_ib_j)]$ where the b_i's are reciprocal lattice vectors.

c) $Na_{.875}K_{.125}VO_3$

Monoclinic F.W. = 123.94

a = 10.533(2) Å

b = 9.580(2) Å

c = 5.850(1) Å

β = 107.56(1)°

V 562.83 Å^3

Z = 8

Dx = 2.93 g/cm^3

Space group: C2/c

Systematic absences: h+k odd, in general

h0ℓ ℓ odd

$Na_{0.5}K_{0.5}VO_3$ positional parameters were used to initiate the refinement. The final discrepancy factors were:

$$R = 0.032$$

$$R_w = 0.039$$

and weights were set equal to:

$$w = [3.0 + 0.03k|F_o| + 0.0004(k|F_o|)^2 + 300(\sigma[F_o]/|F_o|)^2]^{-1} \quad (4.3)$$

The refined secondary extinction parameter was $2.7(7) \times 10^{-7}$. The final positional and thermal parameters are listed in Table 4.3a and Table 4.3b respectively.

TABLE 4.3a

Positional parameters for $Na_{.875}K_{.125}VO_3$ with standard deviations in parentheses

ATOM	x	y	z
V	.29110(7)	.08893(8)	.2528(1)
M1†	0	.9104(3)	1/4
M2††	0	.2980(4)	1/4
O1	.1280(3)	.0984(4)	.1643(6)
O2	.3533(4)	.2448(4)	.3165(7)
O3	.3508(3)	.0108(4)	.0248(6)

† M1 = Na

†† M2 = 0.75(3) Na + 0.25K

TABLE 4.3b

** Thermal parameters for $Na_{.875}K_{.125}VO_3$

with standard deviations in parentheses

ATOM	U(1,1)	U(2,2)	U(3,3)	U(1,2)	U(1,3)	U(2,3)
V	.0129(4)	.0194(5)	.014(5)	-.0015(4)	.0041(3)	-.0002(3)
M1 †	.017(1)	.023(2)	.020(1)	0	.003(1)	0
M2 ††	.033(2)	.0278(2)	.028(2)	0	-.008(2)	0
O1	.013(2)	.030(2)	.021(2)	.0002(14)	.004(1)	.002(2)
O2	.027(2)	.029(2)	.031(2)	-.008(2)	.008(2)	-.002(2)
O3	.021(2)	.035(2)	.021(2)	-.002(2)	.006(1)	-.006(2)

† M1 = Na

†† M2 = .75(3) Na + .25K

** The expression for the temperature factor is $\exp[-2\pi^2(\sum_{i=1}^{3}\cdot\sum_{j=1}^{3} U_{ij}h_ih_jb_ib_j)]$ where the b_i's are reciprocal lattice vectors.

4.1.3. Description of the Structures

a) $NaV_{2/3}P_{1/3}O_3$

$NaV_{2/3}P_{1/3}O_3$ has a modified diopside structure, similar to that of α-$NaVO_3$ (Marumo et al., 1974). VO_4 tetrahedra share corners to form infinite chains parallel to c (Figure 4.1). The Na lie on two non-equivalent special positions, which are characteristic of the monoclinic pyroxenes (Section 1.3.1). The smaller M1 sites are octahedrally co-ordinated and form chains parallel to c. Adjacent octahedra share an O1-O1 edge. The tetrahedral and octahedral chains are linked by corner-sharing between every third octahedron and every third tetrahedron. The larger M2 sites are irregularly six-fold coordinated and serve as a further link between the octahedral and the tetrahedral chains.

The structure is based on staggered layers, roughly perpendicular to a^*. Both the M1 and the M2 sites lie on the same level, and they are linked to tetrahedral chains at slightly higher and slightly lower levels. The layers are stacked on top of each other by the C-centering operation.

The average V-O bond distance is 1.681 Å (Table 4.4). The V-O3 distances are the longest at 1.765(3) and 1.759(3) Å, despite the fact that both O3 and O2 are bonded to three cations and O1 is bonded to four cations. r(V-O1) and r(V-O2) are significantly shorter at 1.608(?) and 1.592(2) Å. The tetrahedral angles range from 105.4(1)° to 111.6(1)°. The average Na1-O bond distance is 2.349 Å. The shortest bond is r(Na1-O2) at 2.303(3) Å, and the longest bond is r(Na1-O1(1)) at 2.377(3) Å, a spread of 0.074 Å.

The average Na2-O bond distance is 2.507 Å, counting only the six oxygens lying within 3 Å of the cation. Bond distances vary from 2.407(3) Å

Figure 4.1 The Structure of $NaV_{2/3}P_{1/3}O_3$

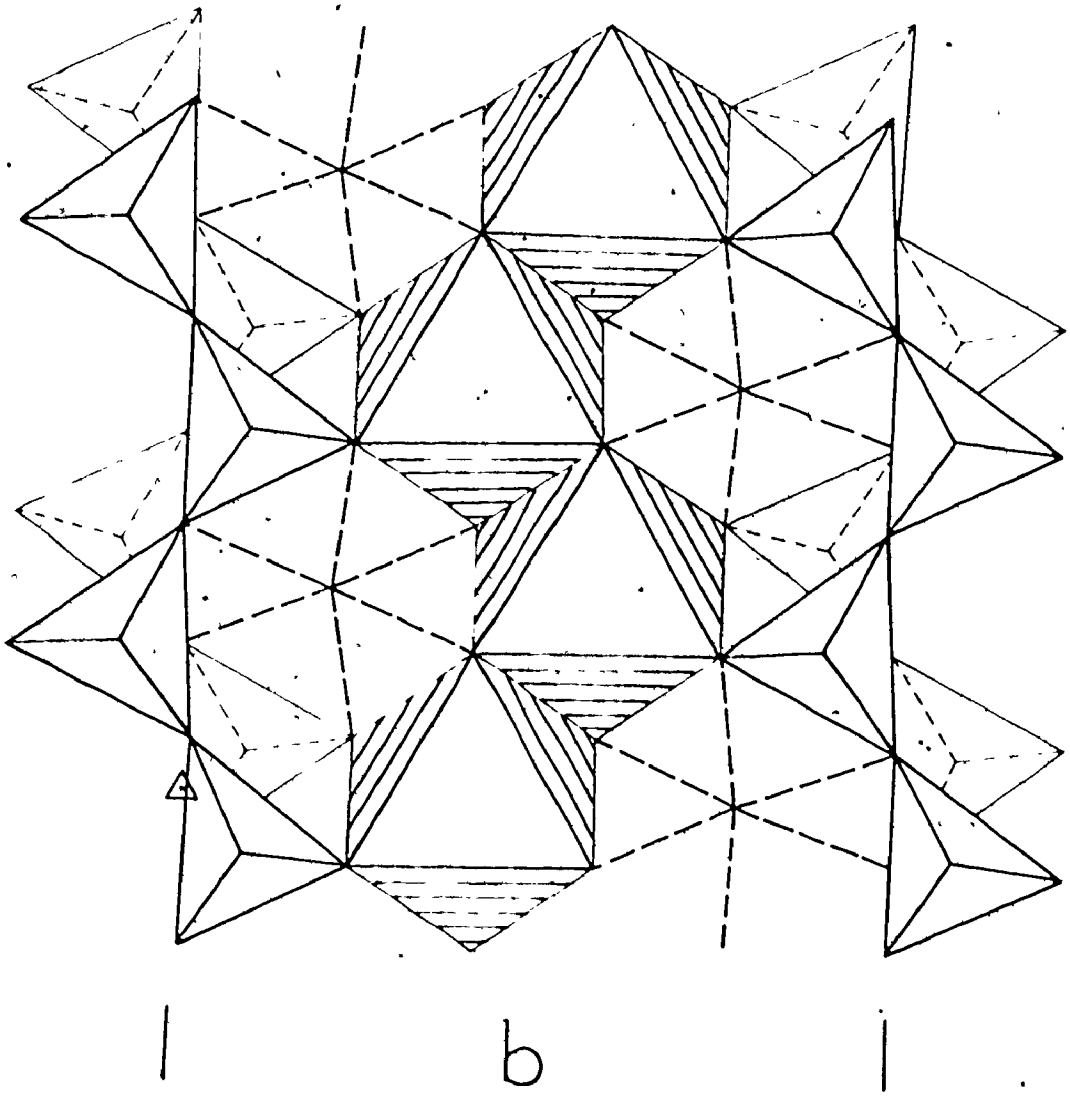

△ unit cell origin

TABLE 4.4

Bond distances and bond angles in $NaV_{2/3}P_{1/3}O_3$ with standard deviations in parentheses

Bond	Distance (Å)	
M1† -O1(2)	2.368(2)	2x
-O1(1)	2.377(3)	2x
-O2	2.303(3)	2x
<M1-O>	2.349	
M2†† -O1	2.407(3)	2x
-O2	2.469(2)	2x
-O3(5)	2.646(3)	2x
<M2-O>	2.507	
X* -O1	1.608(2)	
-O2	1.592(2)	
-O3(1)	1.764(3)	
-O3(4)	1.759(3)	
<X-O>	1.681	

Bonds	Angle (deg.)
O1(2)-M1-O1(4)	176.9(1)
-O1(1)	90.49(8)
-O1(3)	91.87(8)
-O2(5)	87.68(8)
-O2(7)	90.17(8)
O1(1)-M2-O1(3)	80.7 (1)
-O2(6)	83.35(8)
-O2(8)	85.45(8)
-O3(5)	141.90(8)
-O3(7)	113.41(7)
O1(1)-X-O2	110.6 (1)
-O3(1)	110.7 (1)
-O3(4)	111.6 (1)
O2-X-O3(1)	109.7 (1)
-O3(4)	105.4 (1)
O3(1)-X-O3(4)	108.6 (1)
O1(1)-M1-O1(3)	81.87(9)
-O2(5)	174.1 (1)
-O2(7)	92.53(8)
O2(5)-M1-O2(7)	93.1 (1)
O2(6)-M2-O3(5)	131.0 (1)
-O3(7)	62.77(8)
-O2(8)	165.3 (1)
O3(5)-M2-O3(7)	78.08(9)
O3(4)-O3(1)-O3(4)	173.4 (1)

† M1 = Na

†† M2 = Na

* X = .658(4) V + .342 P

Note: The position of atom A(n) is derived from that of atom A(1) by the n^{th} symmetry operation as it appears in the International Tables for X-ray Crystallography, Vol. I, 101 (1965). For example, O1(2) is related to O1(1) by the operation of the center of symmetry at the origin.

for r(Na2-O1) to 2.646(3) Å for r(Na2-O3(5)), a range of 0.239 Å. The difference between the longest bonding distance and the shortest non-bonding distance, r(Na2-O3(6)), is 0.537 Å.

b). $Na_{0.5}K_{0.5}VO_3$

$Na_{0.5}K_{0.5}VO_3$ has the true diopside structure, and differs from α-$NaVO_3$, $LiVO_3$, and $NaV_{2/3}P_{1/3}O_3$ in that the M2 site is irregularly eight-fold coordinated. The cation distribution is ordered, with Na^+ occupying the M1 site and K^+ occupying the M2 site (Figure 4.2). The average V-O bond distance is 1.722 Å (Table 4.5). The V-O3(4) distance is the largest at 1.808(3) Å, and r(V-O2) is the shortest at 1.632(3) Å. In this structure O1 and O3 are bonded to four cations and O2 is bonded to only three. The range of tetrahedral angles in the VO_4 tetrahedron is 106.8(1)° to 110.8(1)°.

The average Na-O bond distance is 2.398 Å. The bond distances vary from r(Na-O1(2)) at 2.386(3) Å to r(Na-O1(1)) at 2.411(4) Å, a spread of 0.025 Å. Thus the M1 octahedron is larger but more regular than that in $NaV_{2/3}P_{1/3}O_3$.

The mean K-O1 distance is 2.780 Å, averaged over the six shortest bond distances only, and 2.822 Å including the next two bond distances. The six shortest bonds range from r(K-O1) at 2.687(3) Å to r(K-O3(5)) at 2.835(3) Å. r(K-O3(6)) is 2.946(3) Å, which is only 0.111 Å greater than r(K-O3(5)). This is much smaller than the corresponding difference of 0.537 Å in $NaV_{2/3}P_{1/3}O_3$.

Figure 4.2 The Structure of $Na_{0.5}K_{0.5}VO_3$

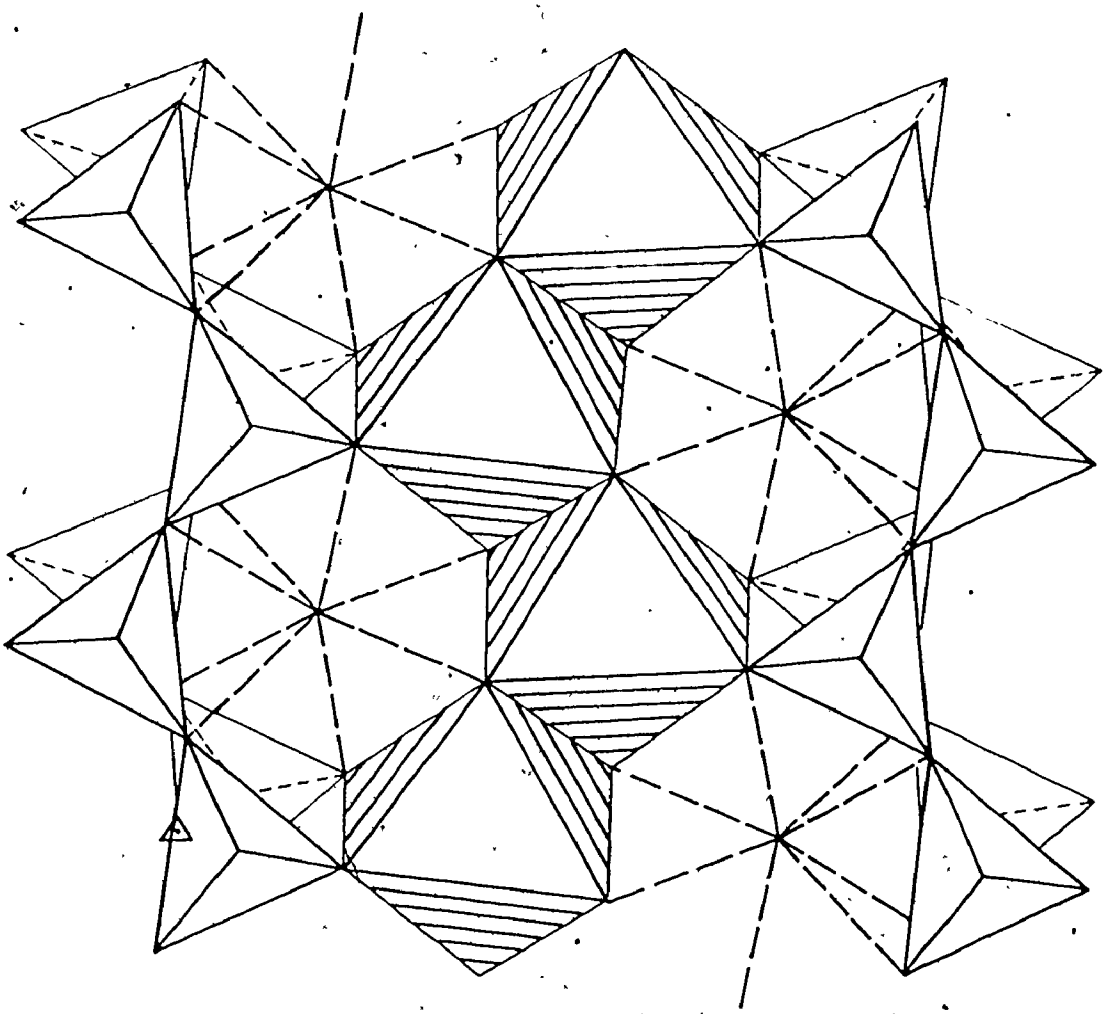

c

b

△ unit cell origin

TABLE 4.5

Bond distances and bond angles in $Na_{0.5}K_{0.5}VO_3$

with standard deviations in parentheses

Bond	Distance (Å)	
M1†-O1(2)	2.386(3)	2x
-O1(1)	2.411(4)	2x
-O2	2.398(4)	2x
<M1-O>	2.398	
M2††-O1	2.687(3)	2x
-O2	2.818(3)	2x
-O3(5)	2.835(3)	2x
-O3(6)	2.946(3)	2x
<M2-O>†*	2.780	
<M2-O>**	2.822	
V-O1	1.642(3)	
-O2	1.632(3)	
-O3(1)	1.804(3)	
-O3(4)	1.808(3)	
<V-O>	1.722	

Bonds	Angle (deg.)
O1(2)-M1-O1(4)	176.9 (2)
-O1(1)	87.3 (1)
-O1(3)	90.3 (1)
-O2(5)	83.1 (1)
-O2(7)	99.1 (1)
O1(1)-M1-O1(3)	80.6 (1)
-O2(5)	169.5 (1)
-O2(7)	95.0 (1)
O2(5)-M1-O2(7)	90.8 (2)
O1(1)-M2-O1(3)	70.9 (1)
-O2(6)	82.63(9)
-O2(8)	82.74(9)
-O3(5)	136.51(8)
-O3(7)	117.81(8)
-O3(6)	92.21(9)
-O3(8)	160.0 (1)
O2(6)-M2-O3(5)	138.7 (1)
-O3(7)	58.53(9)
-O3(6)	106.24(9)
-O3(8)	84.73(9)
-O2(8)	162.0 (1)

† M1 = Na

†† M2 = K

†* includes six shortest bonds

** includes eight shortest bonds

Continued.....

TABLE 4.5 (Continued)

Bonds	Angle (deg.)
03(5)-M2-03(7)	85.92(9)
03(4)-03(1)-03(4)	168.0 (2)
01(1)-V-02	110.3 (2)
-03(1)	110.6 (1)
-03(4)	110.8 (2)
02-V-03(1)	110.5 (2)
-03(4)	106.8 (1)
03(1)-V-03(4)	107.8 (1)

c) $Na_{.875}K_{.125}VO_3$

The structure of $Na_{.875}K_{.125}VO_3$ is of the α-$NaVO_3$ type (Figure 4.3), having both M1 and M2 six-coordinated. All M1 sites are occupied by Na^+, with the rest of the metal cations in M2 sites. The average V-O distance is 1.717 Å (Table 4.6). The actual bond lengths range from 1.628(4) Å for r(V-O2) to 1.801(4) Å for r(V-O3(1)). O1 is bonded to four cations, two M1, one M2, and V. O2 is bonded to M1, M2, and V, and O3 is bonded to M2 and two V. The tetrahedral angles range from 106.0(2)° to 111.2(2)°. The average M1-O distance is 2.371 Å, with M1-O2 the shortest bond at 2.328(4) Å and M1-O1(2) the longest bond at 2.393(3) Å, a range of 0.065 Å. All four M1-O1 bonds are identical within the limits of uncertainty.

The average M2-O distance, including only the six shortest bonds, is 2.572 Å. These six bond distances range from r(M2-O1) at 2.476(5) Å to r(M2-O3(5)) at 2.667(5) Å. r(M2-O3(6)) (3.151(4) Å) is too long to allow O3(6) to be included in the M2 coordination polyhedron. The difference between the longest bonding and the shortest non-bonding distance is 0.484 Å.

4.2. DISCUSSION

The effect of cation substitution in the alkali metavanadate clinopyroxenes may now be discussed, using the structural data obtained during the present study and previous studies of $LiVO_3$ and $NaVO_3$. The $NaVO_3$ data of Marumo et al. (1974) were used since their refinement seems to be the most satisfactory. Data pertinent to the following discussions are summarized in Table 4.7.

Figure 4.3 The Structure of $Na_{.875}K_{.125}VO_3$

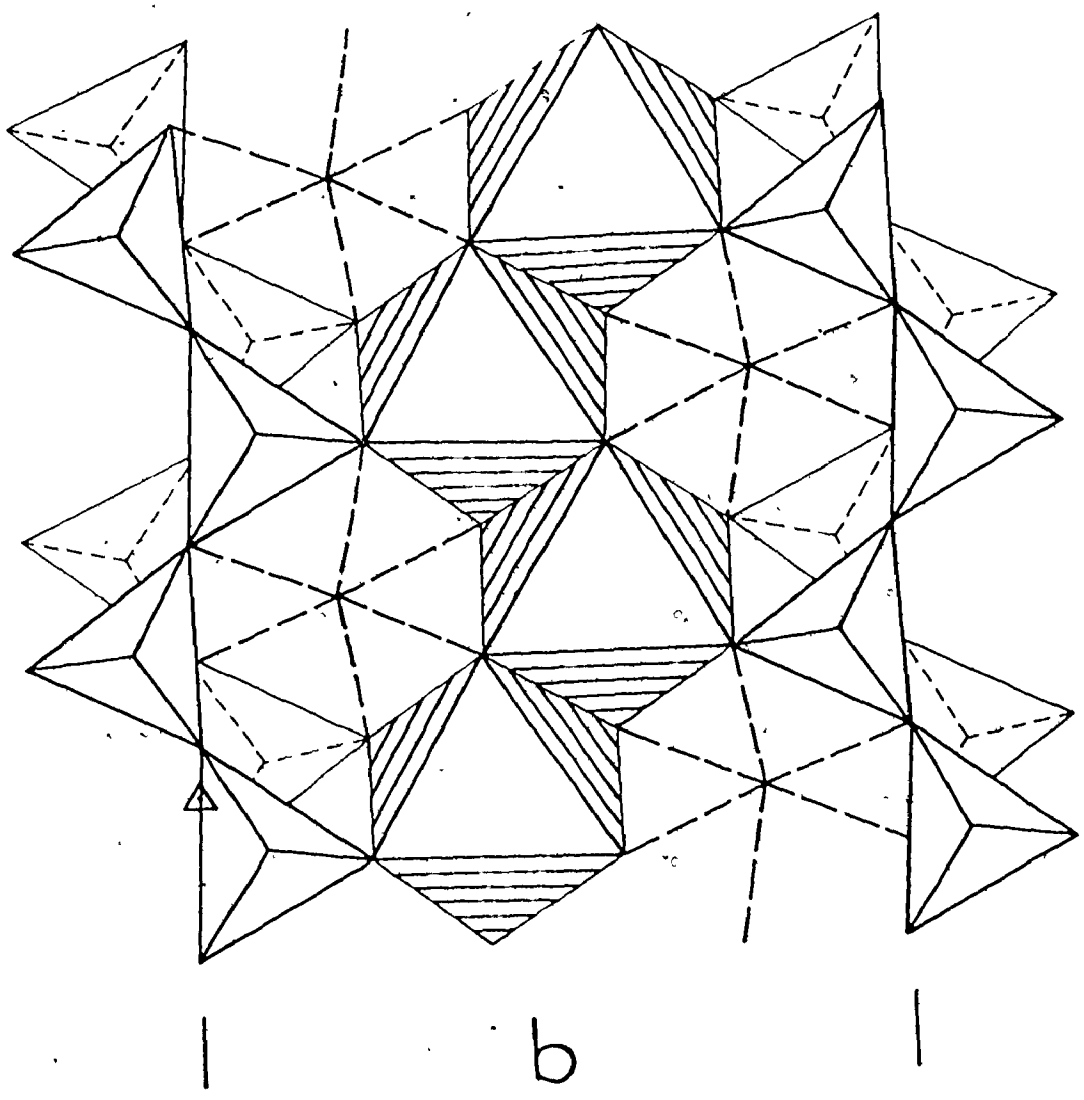

△ unit cell origin

TABLE 4.6

Bond distances and bond angles in $Na_{.875}K_{.125}VO_3$

with standard deviations in parentheses

Bond	Distance (Å)	
M1†-O1(2)	2.393(3)	2x
-O1(1)	2.392(4)	2x
-O2	2.328(4)	2x
<M1-O>	2.371	
M2††-O1	2.476(5)	2x
-O2	2.573(3)	2x
-O3(5)	2.667(5)	2x
<M2-O>	2.572	
V-O1	1.641(3)	
-O2	1.628(4)	
-O3(1)	1.801(4)	
-O3(4)	1.799(4)	
<V-O>	1.717	

† M1 = Na

†† M2 = .75(3) Na + .25 K

Bonds	Angle (deg.)
O1(2)-M1-O1(4)	176.0(2)
-O1(1)	89.7(1)
-O1(3)	93.3(1)
-O2(5)	86.9(1)
-O2(7)	90.4(1)
O1(1)-M1-O1(3)	82.3(2)
-O2(5)	173.1(1)
-O2(7)	91.9(1)
O2(5)-M1-O2(7)	94.1(2)
O1(1)-M2-O1(3)	78.9(2)
-O2(6)	82.8(1)
-O2(8)	83.1(1)
-O3(5)	140.0(1)
-O3(7)	114.5(1)
O2(6)-M2-O3(5)	134.2(2)
-O3(7)	63.0(1)
-O2(8)	161.7(2)
O3(5)-M2-O3(7)	80.3(2)
O3(4)-O3(1)-O3(4)	171.9(2)
O1(1)-V-O2	109.4(2)
-O3(1)	110.9(2)
-O3(4)	111.2(2)
O2-V-O3(1)	110.2(2)
-O3(4)	105.9(2)
O3(1)-V-O3(4)	109.1(2)

TABLE 4.7

Some Structural Data for Alkali Metavanadate Clinopyroxenes

	$LiVO_3$[1]	$NaVO_3$[2]	$NaV_{2/3}P_{1/3}O_3$[3]	$Na_{.875}K_{.125}VO_3$[3]	$Na_{0.5}K_{0.5}VO_3$[3]
<M1-O> (Å)	2.153	2.364	2.349	2.377	2.398
<M2-O> (Å)	2.284	2.513	2.507	2.572	2.780
$\frac{<X-O>}{<M2-O>}$	0.755	0.685	0.671	0.667	0.619
Tetrahedral chain displacement[4] (Å)	1.927	1.435	1.324	1.238	0.625
b(Å)	8.417	9.468	9.475	9.580	9.997
β(deg.)	110.48	108.47	107.62	107.56	104.17
180°-∠O3-O3-O3[5] (deg.)	-19.2	5.5	6.6	8.7	12.0
δ-ε(deg.)[5]	-8.1	2.6	3.7	3.9	5.9

1. Shannon and Calvo, 1973. 2. Marumo, Isobe and Iwai, 1974. 3. This work
4. Tetrahedral chain displacement = $2[cz_{O3} - a \cos \beta\ (0.5 - x_{O3})]$.
5. A negative value indicates S rotation.

Starting with $LiVO_3$, the most obvious effect of substitution by a large cation in the M2 site is an increase in the size of the site. This is shown by a progressive increase in the average M2-O distance from 2.284 Å in $LiVO_3$ to 2.780 Å in $Na_{0.5}K_{0.5}VO_3$. Although the average M1-O distance increases from 2.153 Å in $LiVO_3$ to 2.364 Å in $NaVO_3$, the introduction of a larger cation K^+ results in only a slight increase in <M1-O> since K^+ is found to preferentially occupy the larger M2 site. Presumably the M1 site expands slightly to accomodate the expansion of the M2 site. This expansion of the M2 site can be shown to be accomplished by two simultaneous movements of the rather rigid tetrahedral chains characteristic of the pyroxene structures. These involve the rotation of the tetrahedra to adopt a different chain configuration and the decrease in the so-called back-to-back chain displacement in the c direction.

Thompson (1970) showed that the tetrahedral chains in pyroxenes can adopt two distinct orientations with respect to the octahedral chains. Beginning with a straight, or extended chain, with ∠O3-O3-O3 = 180°, the tetrahedra are rotated about axes normal to the layers and passing through the oxygens linking the tetrahedra to the octahedra. If the tetrahedron rotates so that the triangular face normal to the rotation axis is oriented similarly to the nearest parallel faces of the three octahedra to which the tetrahedron is joined by the oxygen on the rotation axis, the chain is termed S rotated (Figure 4.4). Rotation in the opposite sense results in an O rotated chain. Rotation of each tetrahedron by 30° in the S sense results in hexagonal close packing of oxygens (ABAB), and rotation by 30° in the O sense results in cubic close

Figure 4.4 S, O and E Rotated Pyroxene Chains

a) an O rotated chain

b) an S rotated chain

c) an extended or E chain

After Hawthorne and Calvo (1977).

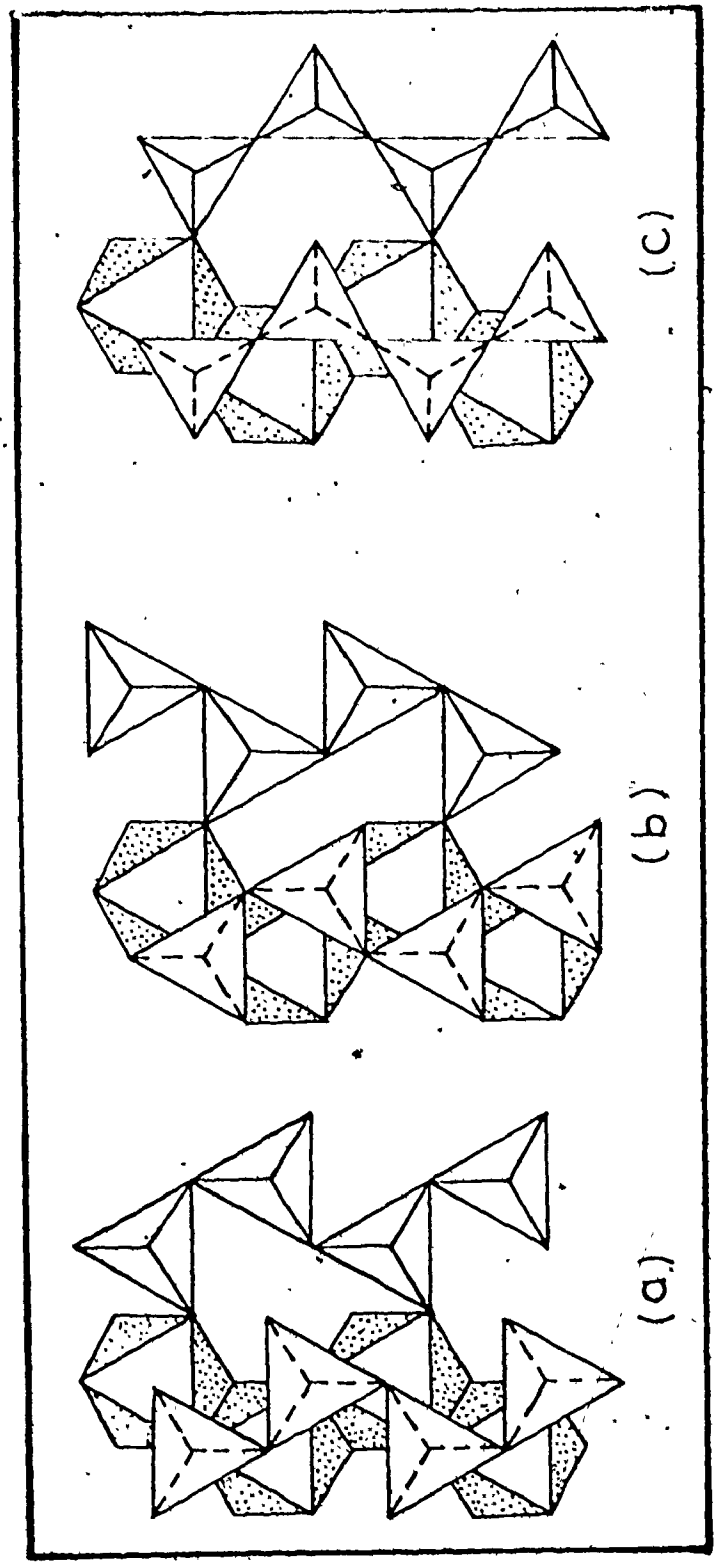
(c)
(b)
(a)

packing of oxygens (ABCABC) (Papike, Prewitt, Sueno and Cameron, 1973). A completely kinked or rotated chain of either type has a chain angle of 120° and the ratio of the tetrahedral to the octahedral edge is 1:1. Papike et al. (1973) have pointed out that the extended, or E chain represents a third possible orientation of the octahedral and tetrahedral chains. The E chain has a chain angle of 180° and the ratio of the tetrahedral edge to the octahedral edge is $\sqrt{3}:2$ (Figure 4.4).

Hawthorne and Calvo (1977) have pointed out that orthorhombic metavanadate pyroxenes have E chains, while the previously known monoclinic metavanadate pyroxenes have kinked chains.

It is possible to differentiate quantitatively between S and O rotated chains by determining the orientations of octahedral and tetrahedral faces with respect to the c axis. The criterion used is illustrated by Figure 4.5. The angle ϵ is subtended by the O1-O1(4)' edge of the M1 octahedron and a vector parallel to the c axis. δ is subtended by a vector parallel to the c axis and the projection of the O1-O3(4) edge of the tetrahedron on the bc plane. O1(4) and O3(4) are related to O1 and O3 by the c glide operation. For E chains $\delta-\epsilon$ is 0°, for complete O rotation $\delta-\epsilon$ is 30°, and for complete S rotation $\delta-\epsilon$ is -30°. For real structures $\delta-\epsilon$ ranges between 0 and 30° for O rotation and between 0 and -30° for S rotation. It can be seen from Table 4.7 that $LiVO_3$ is the only compound in this series with an S rotated chain. This is consistent with the observation by Papike et al. (1973) that in the silicate pyroxenes, an S rotation tends to decrease the size of the M2 site while an O rotation tends to increase it.

Figure 4.5 Criteria for Differentiating Between S and O Rotated Pyroxene Chains

a) angles characteristic of a complete O rotation

b) angles characteristic of a complete S rotation

c) angles characteristic of an extended or E chain

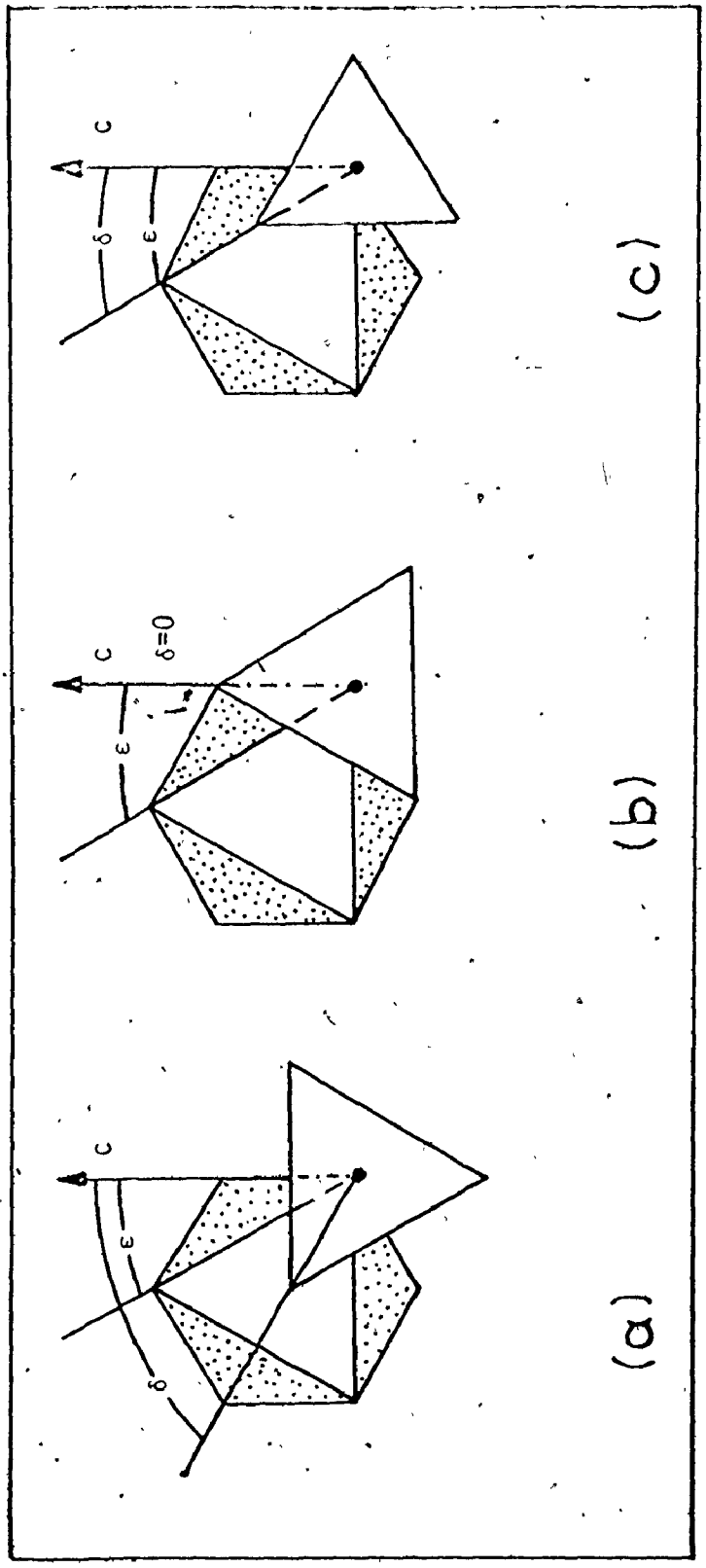
c
δ
ε
(c)
c
δ=0
ε
(b)
c
ε
δ
(a)

Figure 4.6 shows the correlation between the size of the M2 site and the chain rotation as measured by δ-c and the deviation of /03-03-03 from 180°. However, as was pointed out by Hawthorne and Calvo (1977), an S rotation is not necessary to achieve six-fold co-ordination for M2, since $Na_{0.5}K_{0.5}VO_3$ is the only member of this series having an eight-fold coordinated M2 site. The increase in chain rotation should result in an increase in the b axis. This is borne out by the changes in the b axis across the series.

Ohashi and Burnham (1973) have compared the effects of chemical substitution and thermal expansion on the unit cell parameters of several clinopyroxenes between ferrosilite ($FeSiO_3$) and hedenbergite ($CaFeSi_2O_6$). While raising the calcium content produces the same overall results as increasing the temperature, the detailed effects are different. If the degree of deformation due to either chemical substitution or increased temperature is much smaller than the original unit cell parameters, then it can be specified by a second rank tensor (Nye, 1957) which describes the transformation of a sphere in the unstrained body to an ellipsoid in the strained body. The principal axes of the strain ellipsoid are constrained in systems with orthorhombic or higher symmetry. Measurements of the changes in lattice parameters will give the principal strain components exactly. In monoclinic systems one of the principal axes of the strain ellipsoid must be parallel to b. The other two axes, however, are not necessarily parallel to the other two crystallographic axes. Thus measurements of changes in lattice parameters are not sufficient to describe the change in the lattice.

Figure 4.6 Correlation Between Chain Rotation, as Expressed as 180° - ∠03-03-03 and δ-ε, and <M2-0>

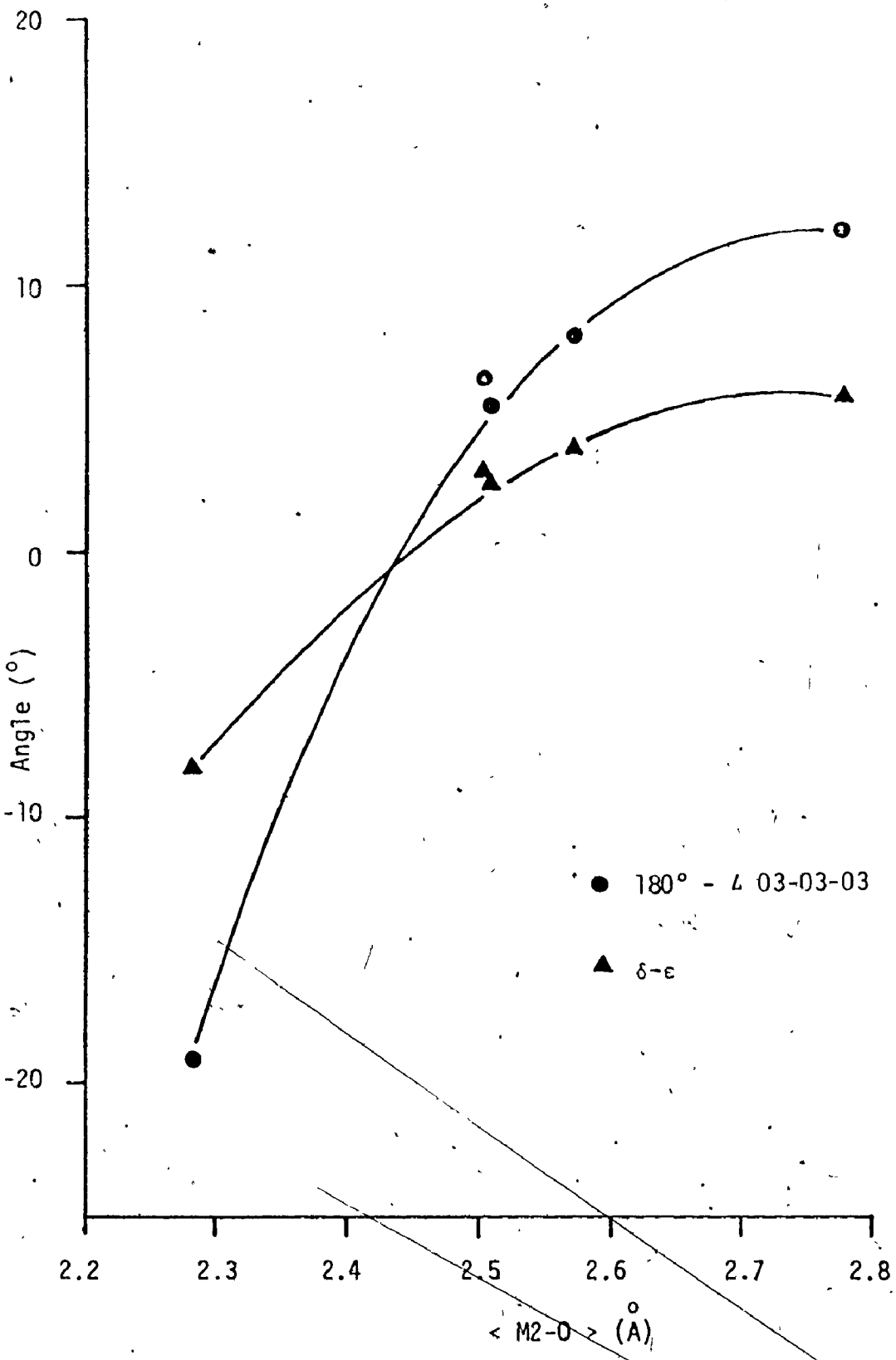
20
10
0
-10
-20
Angle (°)
2.2
2.3
2.4
2.5
2.6
2.7
2.8
< M2-O > (Å)
180° - ∠ 03-03-03
δ-ε

The method of Ohashi and Burnham (1973) has been used to calculate the principal components of the strain tensors for $NaV_{2/3}P_{1/3}O_3$, $Na_{0.5}K_{0.5}VO_3$, and $Na_{.875}K_{.125}VO_3$, using $NaVO_3$ as the unstrained material. In view of the slight but significant discrepancy in the lattice parameters reported by different authors, crystals of $NaVO_3$ were grown and the lattice parameters were measured and used in the calculations. The results are shown in Table 4.8. In each case the greatest lattice expansion lies along b. This expansion is accompanied by a contraction of the a axis relative to $NaVO_3$ in all three structures. The a axis decreases from 10.538 Å in $NaVO_3$ to 10.421 Å in $NaV_{2/3}P_{1/3}O_3$. The decrease upon substitution of 12.5 percent and 50 percent K for Na is of doubtful significance. The b axis shows the greatest increase from 9.444 Å in $NaVO_3$ to 9.997 Å in $Na_{0.5}K_{0.5}VO_3$ while c shows a small but definite decrease from 5.865 Å to 5.804 Å.

Although the size of the cation sites must increase when a larger cation is introduced into the structure, the size of the tetrahedron remains essentially the same. The <V-O> distance varies between 1.717 Å in $Na_{.875}K_{.125}VO_3$ and 1.725 Å in $LiVO_3$. The short <X-O> distance of 1.681 Å in $NaV_{2/3}P_{1/3}O_3$ undoubtedly reflects the substitution of P for V in one-third of the tetrahedral sites, a point which will be dealt with later. The differential expansion of the cation sites in the metavanadate clinopyroxene structure would result in a structural misfit between the tetrahedral and octahedral layers if chain rotation were the only mechanism by which the structure could deal with substitution. This was realized by Cameron et al. (1973) in their study of the effect of

TABLE 4.8

Principal Components of the Strain Tensors for $NaV_{2/3}P_{1/3}O_3$, $Na_{0.5}K_{0.5}VO_3$ and $Na_{.875}K_{.125}VO_3$

	per 1% substitution ($\times 10^{-4}$)			(deg.)		
	ε_1	ε_2	ε_3	Θ_1^*	Θ_2	Θ_3^*
$NaV_{2/3}P_{1/3}O_3$	-1.7	1.0	-8.0	77.5	b	167.5
$Na_{0.5}K_{0.5}VO_3$	9.0	11.7	6.8	56.8	b	146.8
$Na_{.875}K_{.125}VO_3$	11.0	11.5	-1.8	37.5	b	127.5

* Θ_1 and Θ_3 are measured from the positive c direction to the positive a direction.

thermal expansion of some silicate clinopyroxenes. A concomitant displacement of the tetrahedral chains is necessary to accomodate this differential expansion. This mechanism is the so-called "back-to-back" displacement described by Hawthorne and Grundy (1977). It is the relative displacement in the c direction of the chains in adjacent layers. This is measured by the separation of the mid-points of the O3-O3 tetrahedral edges projected onto the bc plane. There is a definite trend in this displacement, which decreases from 1.927 Å in $LiVO_3$ to 0.625 Å in $Na_{0.5}K_{0.5}VO_3$ (Table 4.7).

Since the two chains in question are related by a two-fold rotation in the C2/c structure, a decrease in the chain displacement should be accompanied by a reduction in the β angle. This was found to be true (Table 4.7). The relationship between β and <M2-O> is plotted in Figure 4.7. A similar correlation in the silicate pyroxenes has been pointed out by Papike et al. (1973).

The principal result of P substitution is a decrease in the average X-O bond distance, from 1.723 Å in $NaVO_3$ to 1.681 Å in $NaV_{2/3}P_{1/3}O_3$, and a decrease in <M2-O> and <M1-O>. <Na1-O> is 2.364 Å in $NaVO_3$, and 2.349 Å in $NaV_{2/3}P_{1/3}O_3$. <Na2-O> is 2.513 Å in $NaVO_3$ and 2.507 Å in $NaV_{2/3}P_{1/3}O_3$. The displacement of the back-to-back tetrahedral chains drops from 1.435 Å in $NaVO_3$ to 1.324 Å in $NaV_{2/3}P_{1/3}O_3$. This trend in tetrahedral chain displacement accompanies a trend towards eight-fold M2 coordination. The shortest non-bonding M2-O distance r(M2-O3(6)), drops from 3.239 Å in $NaVO_3$ to 3.183 Å in $NaV_{2/3}P_{1/3}O_3$, although O3(6) is still too far from Na2 to be included in the coordination polyhedron. The tetrahedral chain becomes more kinked, as is shown by the trend in the values of δ-ε and ∠O3-O3-O3.

Figure 4.7 Plot of β versus <M2-O>

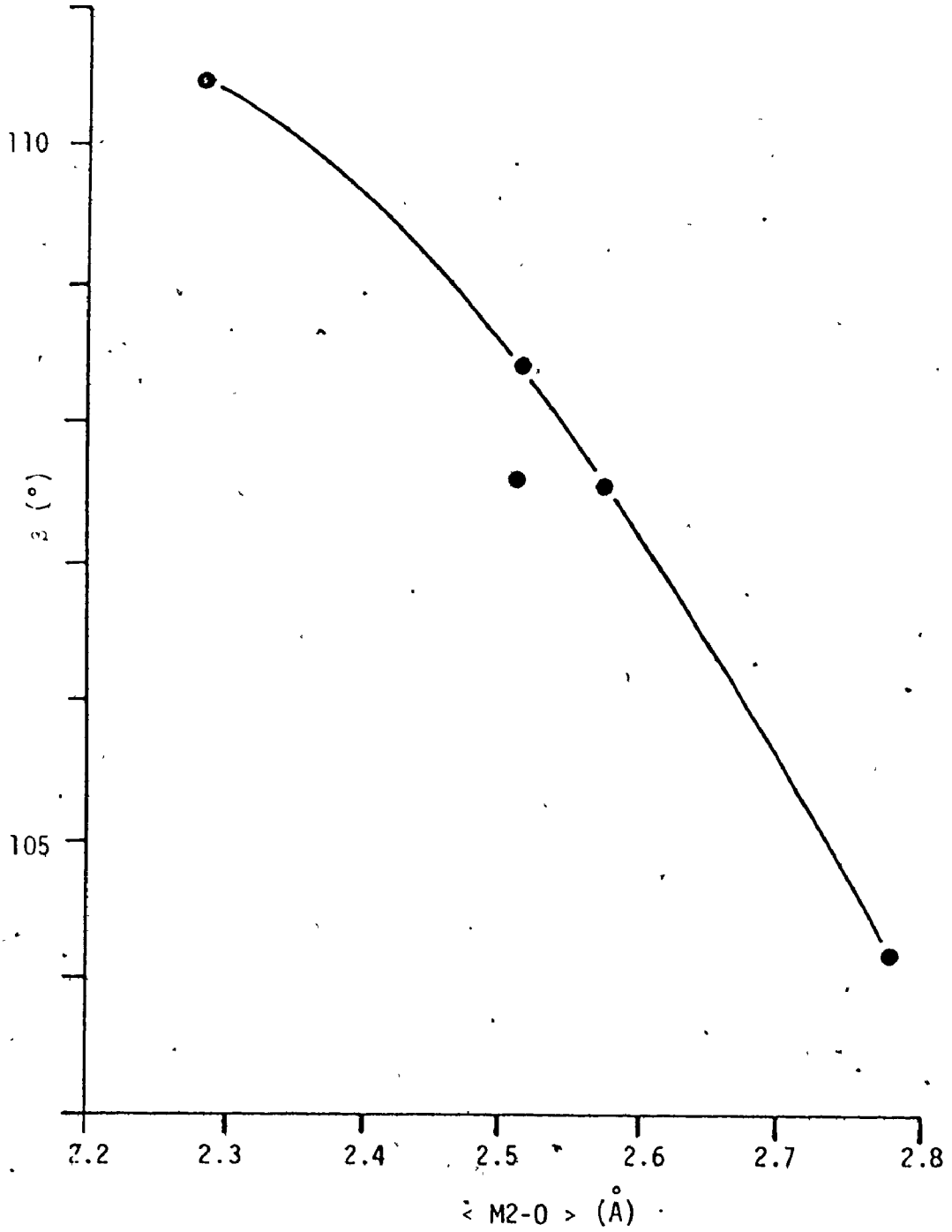
110
105
τ (°)
2.2
2.3
2.4
2.5
2.6
2.7
2.8
< M2-O > (Å)

The fact that decreasing the average size of the tetrahedral site produces effects similar to those resulting from increasing the average size of the M2 site suggests that there may be some correlation between the ratio $\frac{\langle X\text{-}O\rangle}{\langle M2\text{-}O\rangle}$ and some of the observed properties of the pyroxenes. There would seem to be a definite correlation between $\frac{\langle X\text{-}O\rangle}{\langle M2\text{-}O\rangle}$ and β, (Table 4.7) ∠O3-O3-O3, and the tetrahedral chain displacement. Figure 4.8 shows a plot of β versus $\frac{\langle X\text{-}O\rangle}{\langle M2\text{-}O\rangle}$. β, ∠O3-O3-O3, and the tetrahedral chain displacement all decrease as $\frac{\langle X\text{-}O\rangle}{\langle M2\text{-}O\rangle}$ decreases. This correlation would explain why β decreases going from $NaVO_3$ to $NaV_{2/3}P_{1/3}O_3$ despite the normal trend of increasing β with decreasing <M2-O>.

The mechanisms for the expansion of the M2 site discussed previously predict an E chain configuration for some intermediate phase on the $LiVO_3$-$NaVO_3$ join. Such a phase would represent the transition from an S rotated chain in $LiVO_3$ to an O rotated chain in $NaVO_3$. The Na is expected to occupy preferentially the M2 site in such a mixed phase, and the b axis should be shorter than that found in either of the phases having kinked chains. This hypothetical phase might well be orthorhombic, as are most of the known alkali metal metavanadates.

Figure 4.8 Plot of β versus <X-O>/<M2-O>

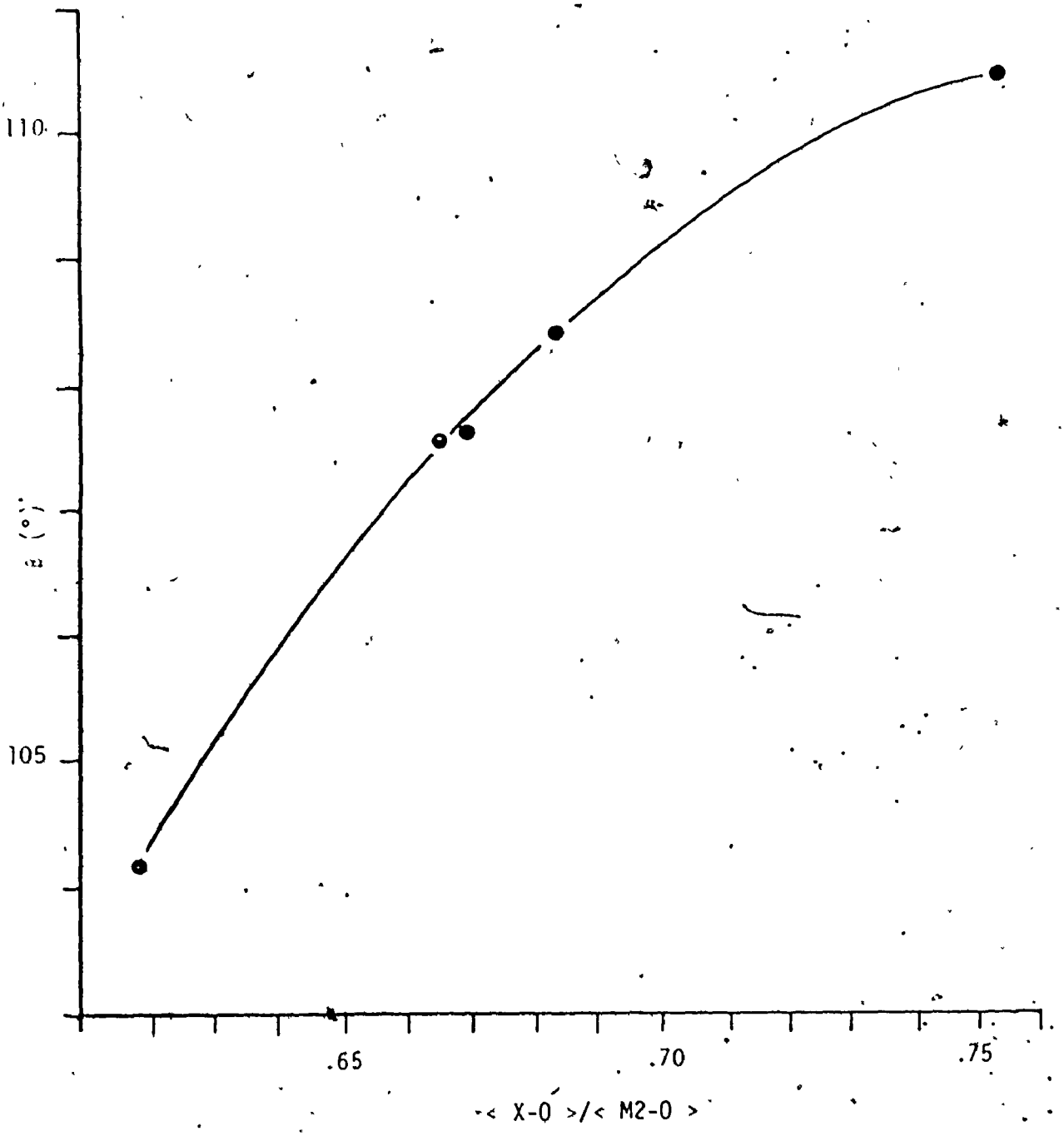
110
105
.65
.70
.75
< X-O >/< M2-O >

CHAPTER 5

CONCLUSIONS AND PROPOSED WORK

5.1. Conclusions

Substantial substitution between pentavalent V and P in tetrahedral sites has been found both in chain and ring structures.

A stable phase with a V:P ratio of 1:3 was found on the $Zn_3(VO_4)_2$-$Zn_3(PO_4)_2$ join. The structure is related to that of α-$Zn_3(PO_4)_2$, but differs from it by the absence of edge-sharing between cation tetrahedra. This may account for the choice of the present structure over that of α-$Zn_3(PO_4)_2$.

Substitution of P for up to one-third of the V in $NaVO_3$ has been observed. The mixed phase has a modified diopside structure and is very similar to that of $NaVO_3$. No evidence has been found for lowering of the space group symmetry or for ordering of V/P.

Substitution of K^+ for Na^+ in the $NaVO_3$ structure has also been studied. A distinctive phase with a Na:K ratio of 1:1 has been found on the $NaVO_3$-KVO_3 join. It has the true diopside structure. Na^+ and K^+ are ordered in the M1 and M2 sites respectively, and the M2 site is irregularly eight-fold coordinated.

The distinctive phase $Na_3K(VO_3)_4$ reported by Perraud (1974) was not found. Instead a solid solution having the composition $Na_{.875}K_{.125}VO_3$ was found. This structure resembles that of $NaVO_3$, and K^+ occupies M2 sites only.

Similar structural changes produced by substitution in both the M and X sites in MXO_3 suggested that the ratio <X-O>/<M2-O> was important in the determination of the characteristics of the structures.

5.2. Proposed Work

At least one other solid solution phase, $Zn_3V_{0.4}P_{1.60}O_8$, has been found on the $Zn_3(VO_4)_2$-$Zn_3(PO_4)_2$ join (Brown and Hummel, 1965). The structure of this phase remains to be determined. It would be most interesting to determine the composition at which the $Zn_3V_{0.5}P_{1.5}O_8$ structure type goes over to the α-$Zn_3(PO_4)_2$ structure type. The determination of the structure of $Zn_3V_{0.4}P_{1.60}O_8$ might give some clue as to where this transition takes place.

The MXO_3 system presents more scope for future work. Structure determinations on the $NaPO_3$ side of the $NaPO_3$-$NaVO_3$ join are hindered by glass formation (Ohashi, 1964) but there is evidence of some crystal formation at high $NaPO_3$ concentrations. Glazyrin (1975) has indicated that there is compound formation on both the $CsVO_3$-$LiVO_3$ and the $CsVO_3$-KVO_3 joins. If these compounds exist their approximate formulae are $Cs_{2/3}Li_{1/3}VO_3$ and $K_{2/3}Cs_{1/3}VO_3$. Several phase changes were indicated in the $CsVO_3$-$LiVO_3$ system. It is not unrealistic to expect that solid solutions may exist in these and other mixed systems.

The next step in the study of the MXO_3 system is the production of non-equivalent X-O chains by substitution in the X and/or the M sites. The most likely candidate to partially replace V^{5+} in the X sites is As^{5+}, isomorphism between the arsenates and the vanadates being well known. Comparing the ionic radii of V^{5+}, P^{5+}, and As^{5+}, it would seem that

substitution between As^{5+}, with an ionic radius of 0.46 Å, and V^{5+} with an ionic radius of 0.59 Å, is much more likely than substitution between V^{5+} and P^{5+}, which has a radius of only 0.35 Å.

There are many possible combinations of M cations which may give rise to solid solution phases. It may be possible to duplicate the structure of ferropigeonite ($(Ca,Mg,Fe)SiO_3$) by preparing a mixed phase containing Na^+ and Li^+.

Ferropigeonite is a clinopyroxene with space group $P2_1/c$ and two types of crystallographically distinct chains (Morimoto et al., 1960). The M cations are Ca^{2+}, Fe^{2+}, and Mg^{2+}. The ratio of the ionic radii of these cations is 1.5:1.2:1.0. A phase containing Na^+ and Li^+ would have a ratio of 1.4:1.0:1.0. There is some possibility that the relative sizes of the M and X cation sites also influence the choice of structure type. The M^{2+}:Si^{4+} radius ratios are 2.24 for Ca^{2+}, 1.81 for Fe^{2+}, and 1.55 for Mg^{2+}. The M^+:V^{5+} ratios in the hypothetical Na/Li phase would be 1.66 for Na^+ and 1.15 for Li^+. If this large difference in the M:X ratios makes it impossible to duplicate the ferropigeonite structure using V^{5+}, substitution of P^{5+} for some V^{5+} may lead to a successful synthesis.

Such a series of syntheses and structure determinations should present an excellent opportunity for determining which factors are most important in determining the choice of structure type.

BIBLIOGRAPHY

Bergman, A.G. and Z.I. Sanzharova; Russ. J. Inorg. Chem., 15, 877 (1970).

Brixner, L.H., R.B. Flippen and W. Jeitschko; Mat. Res. Bull., 10, 1327 (1975).

Brown, J.J. and F.A. Hummel; Trans. Brit. Ceram. Soc., 64, 419 (1965).

Burnham, C.W., J.R. Clark, J.J. Papike and C.T. Prewitt; Zeit. für Krist., 125, 109 (1967).

Calvo, C.; J. Phys. Chem. Solids, 24, 141 (1963).

Calvo, C.; Can. J. Chem., 43, 436 (1965).

Calvo, C.; Bull. Soc. Chim. France, 1744 (1968a).

Calvo, C.; Amer. Mineral., 53, 742 (1968b).

Calvo, C. and R. Faggiani; Unpublished data.

Cameron, M., S. Sueno, C.T. Prewitt and J.J. Papike; Amer. Mineral., 58, 594 (1973).

Clark, J.R., D.E. Appleman and J.J. Papike; Mineral. Soc. Amer. Spec. Publ. 2, 31 (1969).

Deer, W.A., R.A. Howie and J. Zussman; Rock-Forming Minerals, Vol. 2; Longmans, London (1963).

Finger, L.W.; Program and Abstracts, Amer. Crystallogr. Assoc. Winter Meeting, 54 (1969).

Ganne, M., Y. Piffard and M. Tournoux; Can. J. Chem., 52, 3539 (1974).

Glazyrin, M.P.; Dokl. Akad. Nauk SSSR, 221, 91 (1975).

Gopal, R.; Ph.D. Thesis, McMaster University, Hamilton, Ontario (1972).

Gopal, R. and C. Calvo; Can. J. Chem., 49, 3056 (1971).

Gopal, R. and C. Calvo; J. Solid State Chem., 5, 432 (1972).

Hawthorne, F.C. and C. Calvo; Accepted for publication in J. Solid State Chem. (1977).

Hawthorne, F.C. and H.D. Grundy; Can. Mineral., 15, 50 (1977).

International Tables for X-ray Crystallography, Vol. II, J.S. Kasper and K. Lonsdale, Editors; Kynoch Press, Birmingham (1959).

International Tables for X-ray Crystallography, Vol. III, C.H. MacGillavry and G.D. Rieck, Editors; Kynoch Press, Birmingham (1962).

Jordan, B.D. and C. Calvo; Can. J. Chem., 51, 2621 (1973).

Larson, A.C.; Acta Cryst., 23, 664 (1967).

Marumo, F., M. Isobe and S. Iwai; Acta. Cryst., B30, 1628 (1974).

Matsuda, M.; J. Phys. Soc. Japan, 36, 759 (1974).

Morimoto, N., D.E. Appleman and H.T. Evans Jr., Zeit. für Krist., 114, 120 (1960).

Nye, J.F., Physical Properties of Crystals; Oxford University Press, London (1957).

Ohashi, S., In: Topics in Phosphorus Chemistry, Vol. I, M. Grayson and E.J. Griffith, Editors; Wiley, New York (1964).

Ohashi, Y. and C.W. Burnham; Amer. Mineral., 58, 843 (1973).

Papike, J.J., C.T. Prewitt, S. Sueno and M. Cameron, Zeit. für Krist., 138, 254 (1973).

Patterson, A.L.; Zeit. für Krist., 90, 517 (1935).

Pauling, L.; The Nature of the Chemical Bond, Third Edition; Cornell University Press, Ithaca (1960).

Perraud, J.; Revue de Chim. min., 11, 302 (1974).

Prewitt, C.T., A. Sacroug, S. Sueno and M. Cameron; Geol. Soc. Amer. Abs. Prog., 4, 630 (1972).

Ramani, K., A.M. Shaikh, B.S. Reddy and M.A. Viswamitra; Ferroelectrics, 9, 49 (1975).

Sawada, S. and S. Nomura; J. Phys. Soc. Japan, 6, 192 (1951).

Shannon, R.D. and C. Calvo; Can. J. Chem., 51, 265 (1973a).

Shannon, R.D. and C. Calvo; J. Solid State Chem., 6, 538 (1973b).

Stephens, J.S.; Private Communication (1974).

Stephens, J.S. and C. Calvo; Can. J. Chem., 45, 2303 (1967).

Tarte, P.; J. Inorg. Nucl. Chem., 29, 915 (1957).

Thompson, J.B., Amer. Mineral., 55, 292 (1970).

Warren, B.E. and W.L. Bragg; Zeit. für Krist., 69, 168 (1929).

Wilson, A.J.C.; Acta Cryst., 3, 397 (1950).

X-ray 71 System, J.M. Stewart, G.J. Kruger, F.A. Kundell and J.C. Baldwin, Editors; University of Maryland (1971).

Zachariason, W.H.; Acta Cryst., 16, 1139 (1963).

APPENDIX:

STRUCTURE FACTOR TABLES

a) $In_3V_{0.5}P_{1.5}O_8$ Structure Factors

H	K	L	FO	FC	H	K	L	FO	FC	H	K	L	FO	FC
4	0	-4	173	174	-2	0	-4	7	6	3	1	-4	114	118
4	0	-2	291	319	2	0	-8	43	42	7	-1	-6	50	50
8	0	-2	162	161	16	0	-10	17	15	5	1	-6	46	44
6	0	-4	24	24	12	0	-4	24	19	9	-1	-8	45	44
2	0	-4	15	3	-4	0	-4	157	155	7	1	-8	33	31
4	0	-6	232	228	14	0	-6	96	98	11	-1	-10	23	20
10	0	-8	137	132	-2	0	-6	220	207	9	1	-10	60	59
4	0	0	52	48	2	0	-10	26	34	2	-2	-1	88	87
6	0	-2	66	75	12	0	-2	91	91	0	2	-1	30	29
0	0	-4	197	192	14	0	-4	43	38	4	-2	-3	20	17
10	0	-6	59	67	-4	0	-6	8	5	2	2	-3	98	98
4	0	-8	87	87	18	0	-8	27	26	6	-2	-5	48	48
14	0	-10	102	100	0	0	-10	22	11	8	-2	-7	46	45
6	0	-10	24	13	14	0	-2	53	57	8	2	-9	27	25
6	0	0	227	230	-8	0	-4	43	42	10	2	-11	21	30
10	0	-4	212	217	-6	0	-6	48	52	1	-3	0	10	10
12	0	-6	32	32	18	0	-4	9	8	3	-3	-2	92	91
0	0	-6	23	27	-10	0	-4	33	34	1	3	-2	8	4
14	0	-8	52	52	18	0	-2	30	34	5	-3	-4	95	94
4	0	-10	57	63	18	0	0	14	11	7	-3	-6	88	90
8	0	0	14	15	20	0	-2	75	72	9	-3	-8	16	17
10	0	-2	193	192	-10	0	-8	46	46	7	3	-8	15	24
16	0	-2	254	255	20	0	0	15	12	9	3	-10	40	39
16	0	-8	46	44	-14	0	-6	43	33	2	-4	-1	68	86
0	0	-8	41	32	-20	0	-2	20	18	0	-4	-1	201	192
10	0	0	173	178	1	-1	-1	92	85	4	-4	-3	149	149
-8	0	-2	88	91	3	-1	-3	146	151	2	4	-3	35	31
-6	0	-4	253	247	5	-1	-5	120	121	6	-4	-5	64	65
16	0	-6	71	74	7	-1	-7	57	58	4	4	-5	91	93
-2	0	-8	51	52	9	-1	-9	25	23	8	-4	-7	14	4
12	0	0	18	12	11	-1	-11	44	44	6	4	-7	13	16
-10	0	-2	139	146	0	-2	0	236	220	10	-4	-9	36	46
16	0	-4	117	116	2	-2	-2	252	248	8	4	-9	76	80
18	0	-6	59	60	3	-2	-3	7	39	3	-5	-2	88	87
20	0	-8	100	95	4	-2	-4	42	44	5	-5	-4	113	115
-2	0	-10	105	103	6	-2	-6	28	24	3	5	-4	34	39
14	0	0	53	53	8	-2	-8	35	36	7	-5	-6	93	98
16	0	-2	88	92	10	-2	-10	19	22	5	5	-6	14	11
-12	0	2	148	148	1	-3	-1	132	127	9	-5	-8	27	32
20	0	6	56	64	3	-3	-3	20	18	7	5	-8	30	21
-6	0	-8	96	97	5	-3	-5	84	83	2	-6	-1	139	140
-4	0	10	25	28	7	-3	-7	30	32	0	6	-1	71	69
20	0	-4	42	43	9	-3	-9	49	50	4	-6	-3	52	53
-8	0	-8	46	53	0	-4	0	89	86	2	6	-3	76	76
-16	0	-2	73	70	2	-4	-2	71	68	6	-6	-5	28	29
-12	0	-6	102	103	4	-4	-4	26	23	1	-7	0	12	16
22	0	-2	90	83	6	-4	-6	11	1	3	-7	-2	43	42
-16	0	-4	99	98	1	-5	-1	64	65	1	7	-2	70	61
2	0	-2	155	170	3	-5	-3	48	46	3	7	-4	13	2
6	0	-6	97	101	5	-5	-5	43	41	9	1	-11	63	57
8	0	-8	54	54	7	-5	-7	37	33	7	1	-9	66	65
2	0	0	34	36	0	-6	0	23	20	11	-1	-9	53	55
6	0	-8	78	75	2	-6	-2	19	13	9	-1	-7	127	129
12	0	-10	18	29	4	-6	-4	19	1	3	1	-5	8	8
8	0	-10	84	80	6	-6	-6	18	12	7	-1	-5	230	235
-2	0	-2	61	78	1	-7	-1	12	1	5	-1	-3	158	161
8	0	-4	70	70	3	-7	-3	28	27	-1	1	-1	43	37
2	0	-6	83	86	1	-1	0	114	108	3	-1	-1	96	100
12	0	-8	46	40	3	-1	-2	37	41	2	-2	0	138	131
8	0	-2	182	188	1	1	-2	146	145	4	-2	-2	7	10
-4	0	-2	70	73	5	-1	-4	140	143	6	-2	-4	93	93

H	K	L	FO	FC	H	K	L	FO	FC	H	K	L	FO	FC
2	2	-4	140	141	5	3	-8	20	14	4	4	-8	37	36
8	-2	-6	58	69	7	3	-10	61	57	5	-5	-1	6	10
4	2	-6	75	75	4	-4	-1	61	62	-3	5	-1	89	91
10	-2	-8	45	44	-2	4	-1	73	70	7	-5	-3	34	40
6	2	-8	131	128	6	-4	-3	12	16	9	-5	-5	33	39
12	-2	-10	70	71	0	4	-3	98	100	1	5	-5	51	54
8	2	-10	41	34	2	4	-5	78	80	11	-5	-7	25	13
3	-3	-1	45	39	10	-4	-7	77	85	3	5	-7	28	22
-1	3	-1	63	59	4	4	-7	142	144	4	-6	0	25	23
5	-3	-3	183	179	12	-4	-9	43	42	6	-6	-2	22	20
1	3	-3	27	25	6	4	-9	26	22	-2	6	-2	30	36
7	-3	-5	76	77	3	-5	0	83	80	8	-6	-4	36	34
3	3	-5	92	94	-1	5	-2	70	70	0	6	-4	23	26
9	-3	-7	98	101	7	-5	-4	77	80	10	-6	-6	27	23
7	3	-9	22	24	1	5	-4	86	87	2	6	-6	15	21
2	-4	0	20	2	9	-5	-6	69	69	9	-1	-4	49	53
4	-4	-2	14	12	3	5	-6	14	17	-1	1	-4	105	103
0	4	-2	11	18	5	5	-8	6	18	11	-1	-6	33	39
6	-4	-4	7	5	4	-6	-1	26	19	1	1	-6	59	60
2	4	-4	42	40	-2	6	-1	41	39	13	-1	-8	23	26
4	4	-6	65	67	6	-6	-3	45	49	3	1	-8	29	29
10	-4	-8	29	30	8	-6	-5	7	16	15	-1	-10	26	31
6	4	-8	64	60	2	6	-5	94	94	5	1	-10	29	14
3	-5	-1	56	65	4	6	-7	53	55	-4	2	-1	90	87
5	-5	-3	29	30	3	-7	0	6	5	8	-2	-3	184	185
1	5	-3	50	52	5	-7	-2	47	47	-2	2	-3	128	123
7	-5	-5	51	56	-1	7	-2	75	74	10	-2	-5	15	20
3	5	-5	40	38	1	7	-4	37	34	0	2	-5	10	3
9	-5	-7	12	5	5	-1	-1	91	93	12	-2	-7	57	58
5	5	-7	41	34	-3	1	-1	314	316	2	2	-7	86	92
2	-6	0	28	32	7	-1	-3	110	111	14	-2	-9	25	12
4	-6	-2	18	10	-1	1	-3	167	168	4	2	-9	14	10
6	-6	-4	26	31	1	1	-5	151	151	6	2	-11	37	29
2	6	-4	14	18	11	-1	-7	82	80	5	-3	0	108	103
8	-6	-6	14	6	3	1	-7	30	25	7	-3	-2	136	131
4	6	-6	17	23	13	-1	-9	16	11	-3	3	-2	217	208
3	-7	-1	29	22	5	1	-9	24	15	9	-3	-4	42	44
5	-7	-3	7	1	7	1	-11	34	27	-1	3	-4	38	42
1	7	-3	38	26	4	-2	0	128	122	1	3	-6	58	58
3	-1	0	76	74	-2	2	-2	111	110	13	-3	-8	23	26
5	-1	-2	96	99	8	-2	-4	89	92	3	3	-8	28	26
-1	1	-2	173	180	2	2	-6	140	145	5	3	-10	29	25
1	1	-4	16	17	12	-2	-8	78	78	6	-4	-1	164	160
9	-1	-6	75	78	4	2	-8	32	28	-4	4	-1	13	6
3	1	-6	56	65	14	-2	-10	48	45	8	-4	-3	69	66
5	1	-8	67	70	6	2	-10	40	42	10	-4	-5	81	83
13	-1	-10	12	18	5	-3	-1	146	139	0	4	-5	111	114
4	-2	-1	122	113	-3	3	-1	121	118	12	-4	-7	17	8
-2	2	-1	94	91	-1	3	-3	240	234	4	4	-9	25	30
6	-2	-3	29	29	9	-3	-5	72	73	5	-5	0	103	97
0	2	-3	8	7	1	3	-5	3	21	7	-5	-2	73	76
8	-2	-5	58	61	11	-3	-7	12	12	-3	5	-2	143	140
2	2	-5	132	133	13	-3	-9	3	24	9	-5	-4	16	23
4	2	-7	51	54	5	3	-9	60	57	-1	5	-4	58	59
12	-2	-9	56	70	4	-4	0	23	17	11	-5	-6	11	2
6	2	-9	79	75	6	-4	-2	47	50	1	5	-6	43	42
3	-3	0	151	142	8	-4	-4	8	12	6	-6	-1	44	46
-1	3	-2	90	86	0	4	-4	57	60	-4	6	-1	51	54
7	-3	-4	101	98	10	-4	-6	13	21	8	-6	-3	104	104
1	3	-4	131	131	2	4	-6	48	49	-2	6	-3	56	55
11	-3	-8	54	61	12	-4	-8	22	17	0	6	-5	7	16

H	K	L	FO	FC
5	-7	0	89	93
7	-7	-2	24	6
-3	7	-2	56	61
7	-1	-1	149	152
-5	1	-1	58	59
9	-1	-3	37	36
-3	1	-3	151	148
11	-1	-5	38	38
-1	1	-5	34	37
13	-1	-7	86	84
1	1	-7	116	114
3	1	-9	70	68
5	1	-11	73	78
6	-2	0	7	8
8	-2	-2	231	232
-4	2	-2	77	75
10	-2	-4	116	119
-2	2	-4	85	87
12	-2	-6	115	119
2	2	-8	22	19
14	-2	-8	47	44
-5	3	-10	20	2
9	-3	-1	185	179
-3	3	-3	4	42
11	-3	-5	79	82
-1	3	-5	61	61
13	-3	-7	7	2
1	3	-7	10	1
15	-3	-9	44	39
3	3	-9	66	83
-4	4	-2	79	78
10	-4	-2	31	29
12	-4	-4	95	93
14	-4	-6	42	42
7	-5	-8	25	13
9	-5	-1	56	58
-3	5	-3	15	20
11	-5	-3	57	44
-1	5	-5	17	14
13	-5	-7	42	39
1	5	-7	17	28
6	-6	0	35	38
8	-6	-2	15	15
-4	6	-2	42	40
10	-6	-4	29	23
-2	6	-4	7	7
0	6	-6	21	26
7	-7	-1	47	47
-5	7	-1	28	9
-3	7	-3	36	35
9	-7	-3	98	101
-5	7	-2	108	110
11	-7	-4	59	75
-3	7	-4	76	77
-1	7	-6	62	58
15	-7	-8	55	53
3	7	-10	37	45
8	-8	-1	95	92
-6	8	-1	41	38

H	K	L	FO	FC
10	-8	-3	38	42
-4	8	-3	78	77
12	-8	-5	120	123
-2	8	-5	28	31
14	-8	-7	24	14
0	8	-7	39	45
16	-8	-9	20	12
2	8	-9	32	27
4	-9	-11	8	2
7	-9	0	105	103
-3	9	-4	63	65
13	-9	-6	75	78
-1	9	-8	47	50
15	-9	-8	83	81
1	9	-10	30	32
3	-10	-1	75	74
4	-10	-3	21	158
-4	10	-3	24	24
12	-10	-5	49	47
-2	10	-5	94	93
14	-10	-7	58	62
0	10	-7	19	14
7	-11	0	52	55
-3	11	-2	24	22
9	-11	-4	47	48
-5	11	-6	65	70
11	-11	-6	48	50
-1	11	-8	84	84
13	-11	-8	77	79
1	11	-10	17	7
3	-12	-1	57	54
-3	12	-3	71	70
5	-12	-5	26	27
-1	12	-5	5	15
11	-12	-7	9	5
-1	12	-7	63	63
13	-12	-9	109	106
1	12	-9	85	88
3	-13	-11	106	105
-3	13	-11	89	87
5	-13	-1	104	102
-1	13	0	21	27
7	-14	-2	134	132
-5	14	-2	14	7
9	-14	-4	105	102
-3	14	-4	105	104
11	-14	-6	194	193
-1	14	-6	31	30
13	-14	-8	59	58
1	14	-8	23	24
3	-15	-10	41	44
-3	15	-1	45	51
5	-15	-1	91	92
-1	15	-3	54	52
7	-15	-3	39	37
9	-15	-5	6	1
-5	15	-7	87	87
11	-15	-7	103	104
-3	15	-9	34	28
1	15	-9	11	19
8	-16	-2	21	22
10	-16	-4	28	12

H	K	L	FO	FC
-6	4	-2	43	42
12	-4	-4	31	32
-4	4	-4	54	53
14	-4	-6	27	28
-2	4	-6	39	45
0	4	-8	17	10
9	-5	-1	29	33
-7	5	-1	37	43
11	-5	-3	36	38
-5	5	-3	39	37
13	-5	-5	31	29
-3	5	-5	36	33
-1	5	-7	20	30
10	-6	0	22	22
-6	6	-2	17	15
12	-6	-2	7	6
-4	6	-4	5	15
8	-6	-4	11	11
-2	6	-6	15	21
2	-7	-1	23	4
4	-7	-1	0	71
7	-7	-2	63	66
-3	7	-2	122	124
5	-7	-4	52	50
-1	7	-4	56	55
13	-7	-6	61	63
1	7	-6	19	24
3	-8	-8	6	18
-5	8	-8	62	62
9	-8	-10	26	26
-3	8	-1	10	13
11	-8	-1	90	92
-1	8	-3	17	21
13	-8	-3	7	5
1	8	-5	78	76
6	-9	-7	44	45
8	-9	-7	14	8
-4	9	-9	23	25
10	-9	0	83	81
-2	9	-2	37	35
0	9	-6	62	61
7	-10	-8	49	48
-5	10	-8	31	36
9	-10	-10	11	27
-3	10	-1	84	81
11	-10	-3	34	31
-1	10	-3	177	174
13	-10	-5	62	67
1	10	-5	56	60
3	-11	-7	63	67
-3	11	-9	47	42
5	-11	0	82	84
-1	11	-2	54	56
7	-11	-2	33	35
-5	11	-4	39	31
9	-11	-6	22	23
-3	11	-6	26	25
11	-11	-8	66	70
-1	11	-8	37	52
13	-11	-10	97	102
1	11	-10	28	23

H	K	L	FO	FC
-6	6	-3	88	84
-4	6	-5	92	90
11	-1	-1	191	195
-9	-1	-1	130	134
13	-1	-3	150	150
-5	-1	-5	49	53
17	-1	-5	74	75
-3	-1	-7	32	30
-1	-1	-7	72	71
1	-1	-9	24	24
10	-2	-11	20	14
-8	-2	0	41	43
14	-2	-2	153	159
-6	-2	-4	74	73
16	-2	-6	68	67
-4	-2	-6	9	7
16	-2	-8	23	11
-2	-2	-8	19	7
0	-2	-10	40	40
11	-3	-1	150	147
-9	-3	-1	47	49
7	-3	-3	74	76
-5	-3	-5	59	63
15	-3	-5	82	86
-1	-3	-9	37	30
10	-4	0	17	18
14	-4	-4	19	2
16	-4	-6	9	26
-4	-4	-6	26	20
11	-5	-1	20	8
-9	-5	-1	60	64
13	-5	-3	60	56
-7	-5	-5	34	36
15	-5	-5	17	33
-5	-5	-7	32	39
-3	-5	0	24	30
10	-6	-2	18	14
-8	-6	-4	25	25
12	-6	0	60	60
-6	-1	-2	118	119
11	-1	-2	35	35
-9	-1	-4	27	25
13	-1	-4	60	59
-7	-1	-6	40	64
15	-1	-6	31	31
-5	-1	-8	49	49
17	-1	-8	33	27
-3	-1	-10	31	53
19	-1	-1	45	20
-1	-1	-1	100	45
12	-2	-3	62	62
-10	-2	-5	53	54
14	-2	-5	29	27
-8	-2	-7	54	39
16	-2	-7	23	57
18	-2	-9	24	28
-4	-2	0	76	75
2	-3	-2	110	109
11	-3	-2	50	52
-9	-3	-4	50	51

H	K	L	FO	FC
15	-3	-4	42	41
-7	-3	-6	10	6
17	-3	-8	17	15
-3	-3	-10	36	13
12	-4	-1	121	39
-10	-4	-3	18	120
14	-4	-5	88	4
16	-4	-7	78	87
-6	-4	-9	22	80
-4	-4	0	71	17
15	-4	-2	76	69
-2	-4	-4	110	78
11	-5	-2	28	109
13	-5	-4	65	31
-9	-5	-6	7	64
15	-5	-6	54	9
-5	-5	-1	51	51
17	-5	-3	63	48
-11	-5	-3	121	72
0	-5	-5	39	120
-2	-5	-7	97	37
4	-5	-9	68	97
-4	-5	-11	73	70
6	-5	-1	71	71
-6	-6	-1	19	70
8	-6	-3	89	22
-8	-6	-5	33	89
10	-6	-7	91	28
-10	-6	-9	13	92
1	-6	-11	30	7
-1	-6	-1	42	35
3	-6	-3	109	41
-3	-6	-5	16	110
5	-6	-7	74	2
-5	-6	-9	38	73
7	-6	-11	29	39
-7	-7	-1	103	27
9	-7	-3	89	104
-9	-7	-5	14	86
11	-7	-7	86	15
-11	-7	-9	33	88
0	-8	-2	47	34
2	-8	-4	15	53
-2	-8	-6	10	6
4	-8	-8	12	4
-4	-8	-10	42	13
6	-8	-1	16	39
-6	-8	-3	34	17
8	-8	-5	58	26
-8	-8	-7	15	36
10	-8	-9	34	57
-10	-8	-1	15	5
1	-9	-2	34	44
-1	-9	-4	15	17
3	-9	-6	62	21
-3	-9	-8	72	11
5	-9	-10	17	63
-5	-9	-1	62	72
7	-9	-3	72	31

H	K	L	FO	FC
-9	1	-4	6	16
19	-1	-6	17	27
-7	-1	-6	75	77
1	-1	-8	8	5
-5	-1	-10	21	13
3	-1	-5	65	69
-5	-2	-7	28	19
18	-2	-7	29	23
20	-2	-9	60	61
-6	-2	-2	11	13
-4	-2	-4	67	60
15	-2	-6	58	62
-7	-2	-8	30	48
17	-2	-1	9	14
-5	-3	-1	60	55
14	-3	-3	70	61
-4	-3	-5	26	4
16	-3	-5	24	25
-2	-3	-7	44	38
18	-3	0	63	68
-8	-3	-2	29	28
20	-3	-4	35	26
-10	-3	-6	29	27
1	-4	-3	75	79
-1	-4	-5	68	66
3	-4	-1	51	52
-3	-4	-3	53	59
5	-4	-5	66	65
-5	-4	-7	20	15
7	-4	-9	49	52
-7	-4	-11	58	57
9	-4	0	22	27
-9	-4	-2	99	106
11	-4	-4	43	47
-11	-4	-6	32	28
0	-5	-1	62	60
2	-5	-3	131	131
-2	-5	-5	55	50
4	-5	-7	32	37
-4	-5	-9	132	135
6	-5	0	11	7
-6	-5	-2	62	62
8	-5	-4	57	57
-8	-5	-6	69	69
10	-5	-8	26	14
-10	-5	-1	68	69
1	-6	-3	33	31
-1	-6	-5	38	39
3	-6	-7	18	21
-3	-6	-9	24	27
5	-6	-11	82	84
-5	-6	-1	37	31
7	-6	-3	36	44
-7	-6	-5	83	78
9	-6	-7	43	44
-9	-6	0	35	40
11	-6	-2	56	53
-11	-6	-4	3	15
0	-7	-4	17	4
2	-7	-6	7	19
-2	-7	-8	45	39

H	K	L	FO	FC	H	K	L	FO	FC	H	K	L	FO	FC
15	-5	-1	16	29	19	-1	-2	31	29	15	-1	-1	49	51
-13	5	-1	28	27	-15	1	-2	41	42	13	-1	0	29	14
-11	5	-3	18	2	21	-1	-4	49	41	14	-2	-2	29	26
-9	5	-5	37	37	-11	1	-6	25	23	-8	4	-3	28	28
15	-1	0	44	47	-9	1	-8	37	28	-5	3	-6	32	27
17	-1	-2	33	34	18	-2	-1	69	69	-6	4	-4	37	36
-13	1	-2	14	17	20	-2	-3	3	18	12	-4	-2	29	18
19	-1	-4	18	17	-14	2	-3	13	24	-8	4	-2	37	33
-11	1	-4	68	70	-12	2	-5	20	8	13	-3	-3	25	18
21	-1	-6	42	37	-10	2	-7	39	51	12	-2	-2	28	20
-9	1	-6	9	1	17	-3	0	32	27	-8	4	-1	30	9
-7	1	-8	29	24	19	-3	-2	38	36	13	-3	-4	24	22
-5	1	-10	28	24	-13	3	-4	25	9	11	-3	-2	33	33
16	-2	-1	35	31	-11	3	-6	33	26	9	-1	-1	30	33
-14	2	-1	106	106	18	-4	-1	21	23	-5	3	-3	30	28
18	-2	-3	58	62	-16	4	-1	65	68	-5	5	-2	23	13
20	-2	-5	11	17	-14	4	-3	9	2	8	-4	-1	41	38
-10	2	-5	13	12	-12	4	-5	47	45	-1	3	-6	24	23
-8	2	-7	51	46	19	-1	-1	39	40	11	-3	-4	26	18
-6	2	-9	19	15	-17	1	-1	47	33	9	-3	-2	29	30
15	-3	0	28	16	21	-1	-3	44	44	13	-1	-6	28	22
17	-3	-2	6	5	-15	1	-3	74	73	-5	5	-1	25	20
-13	3	-2	88	92	-13	1	-5	27	33	0	4	-6	29	28
19	-3	-4	52	49	-11	1	-7	12	10	-2	4	-4	31	27
-11	3	-4	54	50	18	-2	0	37	38	6	-4	0	48	46
-9	3	-6	53	63	-16	2	-2	22	21	7	-3	-1	22	20
16	-4	-1	90	92	-14	2	-4	58	54	0	2	-6	30	31
-14	4	-1	49	55	-12	2	-6	43	46	-2	4	-3	32	30
18	-4	-3	25	17	-10	2	-8	70	70	-1	5	-3	25	8
-12	4	-3	75	76	19	-3	-1	15	4	3	3	-7	28	14
-10	4	-5	18	21	-17	3	-1	51	51	5	-5	-2	32	36
-8	4	-7	22	13	-15	3	-3	15	6	7	-3	-3	26	28
15	-5	0	17	13	-13	3	-5	61	54	0	2	-4	20	22
-13	5	-2	62	64	-14	4	-4	8	2	10	-2	-6	32	31
-11	5	-4	54	55	19	-1	0	30	21	6	-2	-2	21	9
17	-1	-1	21	14	21	-1	-2	41	37	8	-4	-5	26	26
19	-1	-3	101	102	-17	1	-2	25	48	9	-3	-6	37	39
21	-1	-5	55	53	-15	1	-4	19	14	5	-3	-2	21	20
-11	1	-5	22	20	-13	1	-6	41	42	11	-1	-8	35	31
-9	1	-7	39	37	20	-2	-1	34	29	7	-1	-4	23	14
-7	1	-9	16	17	-18	2	-1	22	6	-1	5	-1	40	32
16	-2	0	54	61	-16	2	-3	9	3	5	3	-7	51	52
18	-2	-2	101	95	-14	2	-5	49	52	0	2	-2	28	22
-14	2	-2	92	37	-12	2	-7	31	23	1	5	-2	35	33
20	-2	-4	16	13	19	-3	0	26	31	3	3	-4	30	20
-12	2	-4	7	8	-17	3	-2	39	46	6	2	-7	57	58
-10	2	-6	51	51	-15	3	-4	50	55	4	2	-5	22	17
-8	2	-8	6	14	21	-1	-1	37	33	7	-7	0	15	11
17	-3	-1	44	43	-19	1	-1	86	82	-5	7	-2	36	37
-15	3	-1	53	55	-17	1	-3	62	69	-3	7	-1	48	43
-13	3	-3	13	21	-15	1	-5	34	28	7	-7	-3	30	25
-11	3	-5	58	63	20	-2	0	54	53	-1	7	-3	25	1
-9	3	-7	21	16	-18	2	-2	24	30	5	-1	0	164	164
16	-4	0	41	43	-16	2	-4	50	43	7	-1	-2	51	52
18	-4	-2	37	27	-14	2	-6	60	65	-3	1	-2	70	66
-14	4	-2	16	19	-17	3	-3	63	69	11	-1	-3	14	9
-12	4	-4	12	10	21	-1	0	54	40					
-10	4	-6	16	1	-19	1	-2	17	11					
-15	5	-1	29	3	-17	1	-4	44	44					
-13	5	-3	36	40	-20	2	-1	23	24					
17	-1	0	39	37	-18	2	-3	26	28					

b) $NaV_{2/3}P_{1/3}O_3$ Structure Factors

H	K	L	FO	FC
3	7	4	26	25
3	7	-4	12	12
3	7	5	16	17
3	7	-6	11	13
3	9	0	14	14
3	9	1	24	24
3	9	-1	15	15
3	9	-2	5	3
3	9	3	38	38
3	9	-3	12	13
3	9	4	7	11
3	9	-4	10	9
3	9	-5	18	16
3	11	0	35	34
3	11	-1	6	9
3	11	2	34	35
3	11	-2	17	18
4	0	2	66	66
4	0	-2	113	117
4	0	4	35	34
4	0	-4	110	112
4	0	6	36	34
4	0	-6	76	75
4	2	1	27	26
4	2	-1	20	20
4	2	2	44	45
4	2	-2	38	37
4	2	3	7	6
4	2	-3	27	27
4	2	-4	9	8
4	2	-5	36	37
4	2	-6	8	3
4	2	-7	27	29
4	4	0	58	59
4	4	1	25	25
4	4	-1	28	28
4	4	2	11	11
4	4	-2	22	22
4	4	3	15	15
4	4	-3	45	44
4	4	4	26	27
4	4	-4	30	31
4	4	5	8	10
4	4	-5	33	34
4	4	-6	26	25
4	4	-7	25	26
4	6	0	36	36
4	6	1	11	11
4	6	-1	18	19
4	6	2	7	7
4	6	-2	42	42
4	6	3	13	14
4	6	-3	13	12
4	6	4	27	28
4	6	-4	66	65
4	6	5	8	8
4	6	-5	15	14
4	6	6	53	52
4	8	0	34	35
4	8	1	14	15
4	8	2	11	10
4	8	-2	11	13
4	8	-3	14	14
4	8	4	8	10
4	8	-5	30	30
4	10	0	24	23
4	10	1	11	12

H	K	L	FO	FC
4	10	-1	20	20
4	10	2	31	30
4	10	-2	33	32
4	10	-3	13	14
4	10	-4	28	28
5	1	0	84	84
5	1	1	40	41
5	1	-1	55	55
5	1	2	84	85
5	1	-2	40	41
5	1	3	22	23
5	1	-3	50	51
5	1	4	36	38
5	1	-4	40	40
5	1	5	17	17
5	1	-5	28	29
5	1	-6	15	15
5	1	-7	17	16
5	3	0	23	23
5	3	1	154	161
5	3	-1	117	121
5	3	2	10	10
5	3	-2	27	27
5	3	3	110	111
5	3	-3	69	69
5	3	4	19	17
5	3	5	61	61
5	3	-5	42	40
5	3	-6	10	10
5	3	-7	35	35
5	5	0	52	54
5	5	1	4	4
5	5	-2	2	2
5	5	3	4	3
5	5	-3	2	2
5	5	4	4	3
5	5	-4	2	2
5	5	5	4	7
5	5	-5	4	4
5	5	6	4	6
5	5	-6	4	4
5	7	0	22	22
5	7	-1	27	27
5	7	2	48	48
5	7	-2	32	32
5	7	3	7	7
5	7	-3	40	41
5	7	4	41	40
5	7	-4	5	3
5	7	5	14	12
5	7	-5	20	21
5	7	-6	18	18
5	7	7	49	48

H	K	L	FO	FC
5	7	1	52	53
5	7	-1	66	67
5	7	2	37	37
5	7	-2	48	47
5	7	3	44	44
5	7	-3	44	43
5	7	4	34	36
5	7	-4	25	25
5	7	-5	31	33
5	7	-6	22	24
5	9	0	17	17
5	9	1	54	53
5	9	-1	49	50
5	9	2	20	19
5	9	-2	8	9
5	9	3	52	52
5	9	-3	27	27
5	9	-4	12	12
5	11	0	34	34
5	11	-1	16	15
5	11	-2	23	21
6	0	0	90	89
6	0	2	16	15
6	0	-2	55	56
6	0	4	11	13
6	0	-4	48	49
6	0	-6	14	13
6	2	1	27	29
6	2	-1	18	19
6	2	2	10	10
6	2	-2	50	50
6	2	-3	24	24
6	2	-3	15	13
6	2	4	6	6
6	2	-5	24	24
6	2	-6	10	10
6	2	-7	25	26
6	4	0	22	23
6	4	1	7	4
6	4	2	7	5
6	4	-2	12	13
6	4	-3	5	3
6	4	4	10	6
6	4	-4	14	14
6	4	-5	13	14
6	6	0	14	15
6	6	-1	9	9
6	6	-2	13	12
6	6	-2	43	45
6	6	3	6	4
6	6	-3	5	3
6	6	-6	9	7
6	8	0	7	6
6	8	1	20	20
6	8	-1	9	8
6	8	2	13	13
6	8	3	15	13
6	8	-3	11	11
6	8	-4	8	10
6	8	-5	17	16
6	10	0	7	10
6	10	-3	10	9
7	1	0	72	73
7	1	1	32	32
7	1	-1	41	42
7	1	2	74	75
7	1	-2	112	116

H	K	L	FO	FC
7	1	3	25	24
7	1	-3	46	46
7	1	-4	25	27
7	1	-5	61	61
7	1	-6	33	33
7	1	-7	39	39
7	3	0	21	20
7	3	1	19	20
7	3	-1	53	54
7	3	-2	14	13
7	3	-3	10	10
7	3	-4	28	27
7	3	-5	59	60
7	3	-6	9	8
7	3	-7	27	25
7	5	0	15	17
7	5	1	115	116
7	5	-1	10	8
7	5	-2	58	57
7	5	-3	92	92
7	5	-4	10	11
7	5	-5	19	20
7	5	-6	73	72
7	5	-7	21	18
7	7	0	37	38
7	7	1	16	19
7	7	-1	31	30
7	7	-2	23	22
7	7	-3	32	31
7	7	-4	13	15
7	7	-5	29	29
7	7	-6	35	33
7	7	-7	27	25
7	9	0	8	7
7	9	1	43	43
7	9	-1	50	51
7	9	-2	12	14
7	9	-3	19	19
7	9	-4	37	37
7	9	-5	12	10
8	0	0	25	28
8	0	-4	9	8
8	2	0	22	24
8	2	1	17	17
8	2	-1	35	35
8	2	-2	32	33
8	2	-3	33	35
8	2	-4	8	7
8	2	-5	37	36
8	2	-6	42	42
8	2	-7	13	14
8	4	0	30	30
8	4	1	7	5
8	4	-1	15	15
8	4	-2	23	24
8	4	-3	18	17
8	4	-4	9	11
8	4	-5	22	21
8	4	-6	23	23
8	4	-7	13	13
8	6	0	12	12
8	6	-1	14	13
8	6	-2	11	10
8	8	0	11	11
8	8	-1	17	20

H	K	L	FO	FC
8	8	-1	27	26
8	8	-3	24	23
8	8	-4	9	8
8	10	-1	17	17
9	1	0	14	16
9	1	1	13	13
9	1	-1	16	16
9	1	-2	13	14
9	1	-2	51	53
9	1	3	13	13
9	1	-3	20	21
9	1	-4	31	32
9	1	-5	26	25
9	1	-6	35	35
9	3	0	14	15
9	3	1	39	40
9	3	-1	75	76
9	3	2	6	5
9	3	-3	24	23
9	3	-4	84	85
9	3	-5	16	17
9	3	5	67	64
9	5	0	18	18
9	5	1	11	9
9	5	-1	10	10
9	5	-2	23	23
9	5	-4	6	5
9	5	-5	9	11
9	7	0	25	26
9	7	1	23	24
9	7	-1	24	24
9	7	-2	15	16
9	7	-2	19	19
9	7	-3	34	33
9	7	-4	30	29
9	9	-1	33	32
9	9	-2	14	14
10	0	0	42	41
10	0	2	71	70
10	0	-2	54	54
10	0	-4	34	34
10	0	-6	41	40
10	2	0	16	15
10	2	1	30	31
10	2	-1	19	19
10	2	-2	29	28
10	2	-2	35	36
10	2	-3	33	34
10	2	-3	11	12
10	2	-4	8	8
10	2	-5	13	15
10	2	-6	10	9
10	4	1	45	45
10	4	-1	35	33
10	4	-1	29	29
10	4	-2	27	26
10	4	-2	19	19
10	4	-3	22	23
10	4	-4	24	23
10	6	-5	19	17
10	6	0	44	43
10	6	1	12	10
10	6	-1	9	8
10	6	-2	22	22
10	6	-4	35	33
10	6	-1	13	14
10	8	-2	12	11

H	K	L	FO	FC
10	8	-3	6	10
11	1	3	16	16
11	1	1	12	9
11	1	-1	9	8
11	1	-2	12	13
11	1	-3	7	4
11	1	-4	24	24
11	1	-5	7	7
11	3	0	7	6
11	3	1	14	14
11	3	-1	9	9
11	3	-3	7	7
11	3	-5	24	24
11	5	0	7	7
11	5	-1	8	7
11	5	-2	18	19
11	5	-4	26	28
11	7	-2	12	12
12	0	0	2	0
12	0	-2	37	37
12	0	-4	11	13
12	2	0	21	19
12	2	1	53	51
12	2	-1	56	56
12	2	-2	29	30
12	2	-3	43	43
12	2	-4	13	15
12	2	-5	30	31
12	4	0	31	29
12	4	-1	40	39
12	4	-2	23	24
12	4	-3	33	32
12	4	-4	28	26
12	6	-2	4	2
12	6	-3	5	5
12	6	-4	4	4
12	6	-4	14	14
12	6	-5	3	3
12	8	-3	4	3
12	8	-4	3	3
12	8	-5	4	4
12	8	-6	3	2
12	10	-4	2	2
12	10	-5	2	2
13	1	-2	4	4
13	1	-3	3	3
13	3	1	3	2
13	3	-1	3	3
13	3	-3	4	5
13	5	0	3	2
13	5	-1	4	4
13	5	-2	3	3
13	7	0	3	2
13	7	-1	3	3
13	9	-2	3	2
13	11	-1	3	2

c) $Na_{0.5}K_{0.5}VO_3$ Structure Factors

H	K	L	FO	FC	H	K	L	FO	FC	H	K	L	FO	FC
0	0	2	232	232	2	8	6	8	10	3	5	-6	67	69
2	0	0	89	95	2	8	-6	14	16	3	5	-7	20	22
2	0	2	17	14	2	10	0	2	2	3	7	0	21	21
2	0	-2	90	92	2	10	1	42	42	3	7	-1	7	4
2	0	4	29	27	2	10	-1	57	57	3	7	2	39	38
2	0	-4	29	28	2	10	2	6	3	3	7	-2	58	59
2	0	6	10	9	2	10	3	54	52	3	7	3	6	9
2	0	-6	16	14	2	10	-3	23	25	3	7	-3	2	6
2	0	-8	30	31	2	10	4	5	7	3	7	4	7	3
2	2	0	94	95	2	10	-4	10	9	3	7	-4	44	43
2	2	1	170	171	2	10	5	36	37	3	7	5	17	17
2	2	-1	197	197	2	10	-5	20	18	3	7	-5	23	24
2	2	2	49	51	2	12	0	48	43	3	7	6	8	8
2	2	-2	47	50	2	12	1	32	33	3	7	-6	49	47
2	2	3	107	108	2	12	-1	21	19	3	7	-7	10	10
2	2	-3	150	148	2	12	2	33	35	3	9	0	30	31
2	2	4	75	72	2	12	-2	39	39	3	9	1	31	30
2	2	-4	19	20	2	12	3	22	20	3	9	-1	42	41
2	2	5	85	84	2	12	-3	24	25	3	9	2	8	11
2	2	-5	48	50	2	12	-4	25	24	3	9	-2	13	16
2	2	6	37	35	3	1	0	112	109	3	9	3	26	24
2	2	-6	3	2	3	1	1	102	101	3	9	-3	45	46
2	2	7	52	53	3	1	-1	107	109	3	9	4	16	16
2	2	-7	10	11	3	1	2	23	21	3	9	-4	24	26
2	2	-8	8	7	3	1	-2	34	37	3	9	5	11	8
2	4	0	19	20	3	1	3	57	58	3	9	-5	62	60
2	4	1	65	63	3	1	-3	96	97	3	9	-6	13	10
2	4	-1	53	53	3	1	4	40	41	3	11	0	13	14
2	4	2	45	44	3	1	-4	108	110	3	11	1	6	4
2	4	-2	31	31	3	1	5	12	17	3	11	-1	12	11
2	4	3	37	35	3	1	-5	69	67	3	11	-2	15	15
2	4	-3	51	51	3	1	6	20	22	3	11	3	1	0
2	4	4	25	23	3	1	-6	59	59	3	11	4	5	3
2	4	-4	3	1	3	1	7	7	3	3	11	-4	29	33
2	4	5	41	41	3	1	-7	42	41	3	11	-5	16	13
2	4	-5	4	5	3	1	-8	44	44	3	13	0	38	38
2	4	6	37	38	3	3	0	64	66	3	13	1	5	8
2	4	-6	14	15	3	3	1	29	26	3	13	-1	13	9
2	4	7	24	25	3	3	-1	41	38	3	13	2	25	27
2	4	-7	16	14	3	3	2	7	5	3	13	-2	35	38
2	6	0	92	92	3	3	-2	11	9	3	13	-3	18	19
2	6	1	27	25	3	3	3	12	10	4	0	0	51	50
2	6	2	76	75	3	3	-3	24	25	4	0	2	139	139
2	6	-2	102	106	3	3	4	36	34	4	0	-2	123	125
2	6	3	3	1	3	3	-4	30	30	4	0	4	107	106
2	6	-3	25	25	3	3	5	24	24	4	0	-4	46	48
2	6	4	43	45	3	3	-5	47	48	4	0	6	83	84
2	6	-4	52	53	3	3	7	31	32	4	0	-6	39	39
2	6	5	6	7	3	3	-7	47	45	4	0	-8	14	16
2	6	6	51	48	3	5	0	65	67	4	2	0	11	9
2	6	-6	9	9	3	5	1	32	33	4	2	1	7	6
2	6	-7	15	15	3	5	-1	33	33	4	2	-1	43	43
2	8	0	11	10	3	5	2	102	104	4	2	2	60	60
2	8	1	71	70	3	5	-2	120	122	4	2	-2	35	33
2	8	-1	109	108	3	5	3	15	14	4	2	3	29	30
2	8	-2	7	7	3	5	-3	44	44	4	2	-3	21	21
2	8	3	59	67	3	5	4	37	36	4	2	4	30	31
2	8	-3	62	65	3	5	-4	92	90	4	2	-4	28	30
2	8	-4	17	15	3	5	5	9	6	4	2	5	42	41
2	8	5	44	44	3	5	-5	25	26	4	2	-5	25	23
2	8	-5	38	39	3	5	6	22	20	4	2	6	29	27

H	K	L	FO	FC
5	9	-5	29	29
5	9	-6	11	4
5	11	0	50	48
5	11	1	13	17
5	11	-1	33	34
5	11	2	42	41
5	11	-2	39	38
5	11	3	16	20
5	11	-3	18	18
5	11	4	24	28
5	13	0	10	14
5	13	-1	22	26
5	13	-2	15	16
6	0	0	94	92
6	0	2	26	25
6	0	-2	103	101
6	0	4	5	7
6	0	-4	119	117
6	0	6	26	27
6	0	-6	61	59
6	0	-8	49	49
6	2	0	24	26
6	2	-1	31	32
6	2	1	31	33
6	2	-2	75	76
6	2	2	41	43
6	2	-3	87	88
6	2	3	14	13
6	2	-4	27	27
6	2	4	13	9
6	2	-5	53	62
6	2	5	15	10
6	2	-6	35	34
6	2	6	17	16
6	4	-7	36	37
6	4	1	19	20
6	4	-1	13	11
6	4	2	16	18
6	4	-2	27	26
6	4	3	35	34
6	4	-3	44	46
6	4	4	36	37
6	4	-4	11	9
6	4	5	23	23
6	4	-5	32	31
6	4	6	14	9
6	4	-6	26	23
6	4	-7	34	33
6	6	0	16	14
6	6	-1	9	12
6	6	1	28	29
6	6	-2	36	37
6	6	2	8	5
6	6	-3	10	11
6	6	3	52	53
6	6	-4	36	36
6	6	4	11	5
6	6	-5	13	12
6	6	5	35	37
6	8	0	8	2
6	8	1	41	41
6	8	-1	2	0

H	K	L	FO	FC
5	1	-1	52	49
5	1	2	66	67
5	1	-2	80	81
5	1	3	8	3
5	1	-3	15	14
5	1	4	28	30
5	1	-4	15	15
5	1	5	14	14
5	1	-5	28	30
5	1	6	8	7
5	1	-6	46	46
5	1	-7	22	22
5	1	-8	28	23
5	3	0	30	32
5	3	1	158	160
5	3	-1	129	133
5	3	2	32	32
5	3	-2	29	30
5	3	3	65	87
5	3	-3	95	97
5	3	4	14	10
5	3	-4	28	28
5	3	5	37	38
5	3	-5	60	59
5	3	6	15	15
5	3	-6	9	10
5	3	-7	50	48
5	5	0	39	37
5	5	1	58	58
5	5	-1	48	49
5	5	2	29	30
5	5	-2	18	17
5	5	3	12	16
5	5	-3	59	60
5	5	4	7	8
5	5	-4	11	12
5	5	5	9	8
5	5	-5	32	32
5	5	6	17	14
5	5	-6	9	10
5	7	0	28	28
5	7	1	70	69
5	7	-1	94	96
5	7	2	53	53
5	7	-2	65	62
5	7	3	55	54
5	7	-3	60	61
5	7	4	17	17
5	7	-4	50	50
5	7	-5	56	58
5	7	-6	34	36
5	7	-7	31	33
5	9	1	35	36
5	9	-1	51	52
5	9	2	3	5
5	9	-2	27	30
5	9	3	22	22
5	9	-3	6	6
5	9	4	8	1

H	K	L	FO	FC
4	0	12	22	23
4	0	-12	33	33
4	0	14	32	31
4	0	-14	75	73
4	0	16	62	63
4	0	-16	55	49
4	2	13	42	39
4	2	-13	11	12
4	2	15	81	81
4	2	-15	39	39
4	4	12	70	68
4	4	-12	34	32
4	4	14	76	76
4	4	-14	12	11
4	4	16	37	37
4	4	-16	19	15
4	6	13	10	11
4	6	-13	34	34
4	6	15	20	21
4	6	-15	32	32
4	8	12	35	34
4	8	-12	35	34
4	8	14	168	168
4	8	-14	24	25
4	8	16	17	18
4	8	-16	35	35
4	10	13	54	52
4	10	-13	4	3
4	10	15	35	35
4	10	-15	6	8
4	12	12	22	19
4	12	-12	11	11
4	12	14	16	14
4	12	-14	17	16
4	12	16	30	28
4	12	-16	11	12
4	14	13	7	8
4	14	-13	15	11
4	14	15	12	2
4	16	12	110	111
4	16	-12	42	42

H	K	L	FO	FC	H	K	L	FO	FC	H	K	L	FO	FC
6	8	2	9	6	1	1	-5	18	18	1	11	1	18	20
6	8	-2	24	21	1	1	6	27	28	1	11	-1	14	12
6	8	3	49	48	1	1	-6	35	38	1	11	2	19	16
6	8	-3	12	10	1	1	7	21	19	1	11	-2	26	28
6	8	4	8	6	1	1	-7	9	8	1	11	3	10	3
6	8	-4	10	13	1	1	-8	38	40	1	11	-3	22	23
0	0	4	147	148	1	3	0	18	23	1	11	4	12	15
0	0	6	45	45	1	3	1	24	20	1	11	-4	43	45
0	2	0	59	66	1	3	-1	95	99	1	11	-5	16	13
0	2	1	111	105	1	3	2	54	54	1	13	0	11	5
0	2	2	42	40	1	3	-2	70	68	1	13	1	9	0
0	2	3	35	34	1	3	3	18	17	1	13	-1	19	20
0	2	4	21	19	1	3	-3	135	136	1	13	2	12	15
0	2	5	4	2	1	3	4	17	20	1	13	-2	8	2
0	2	6	11	11	1	3	-4	13	8	1	13	-3	17	21
0	2	7	6	1	1	3	5	22	22	6	8	-5	21	24
0	4	0	34	37	1	3	-5	111	110	6	10	0	15	14
0	4	1	144	145	1	3	6	14	16	6	10	1	34	33
0	4	2	85	84	1	3	-6	26	26	6	10	-1	8	10
0	4	3	84	94	1	3	7	18	19	6	10	-2	24	21
0	4	4	10	9	1	3	-7	63	66	6	10	-4	28	31
0	4	5	38	37	1	5	0	97	96	7	1	0	81	79
0	4	6	24	24	1	5	1	15	15	7	1	1	50	47
0	4	7	25	25	1	5	-1	53	53	7	1	-1	62	63
0	6	0	135	133	1	5	2	91	92	7	1	2	76	76
0	6	1	22	23	1	5	-2	17	15	7	1	-2	122	125
0	6	2	136	133	1	5	3	25	25	7	1	3	25	25
0	6	3	12	11	1	5	-3	34	35	7	1	-3	52	52
0	6	4	40	38	1	5	4	77	78	7	1	4	23	23
0	6	5	13	14	1	5	-4	18	18	7	1	-4	38	36
0	6	6	28	27	1	5	5	7	1	7	1	5	21	20
0	6	7	6	5	1	5	-5	31	30	7	1	-5	31	29
0	8	0	35	34	1	5	6	50	51	7	1	-6	34	32
0	8	1	74	73	1	5	-6	33	35	7	1	-7	10	15
0	8	2	52	51	1	5	7	4	1	7	3	0	6	0
0	8	3	35	34	1	5	-7	14	16	7	3	1	74	73
0	8	4	22	21	1	7	0	13	11	7	3	-1	89	90
0	8	5	16	16	1	7	1	56	57	7	3	2	31	32
0	8	6	25	25	1	7	-1	58	58	7	3	-2	36	36
0	10	0	78	76	1	7	2	6	5	7	3	3	31	31
0	10	1	29	28	1	7	-2	60	61	7	3	-3	58	57
0	10	2	53	52	1	7	3	19	20	7	3	4	2	8
0	10	3	13	14	1	7	-3	76	78	7	3	-4	4	3
0	10	4	41	42	1	7	4	8	9	7	3	5	18	19
0	10	5	4	10	1	7	-4	42	45	7	3	-5	12	14
0	12	0	56	58	1	7	5	24	23	7	3	-6	21	18
0	12	1	19	19	1	7	-5	50	50	7	3	-7	3	4
0	12	2	45	42	1	7	6	12	10	7	5	0	141	142
0	12	3	16	15	1	7	-6	47	45	7	5	1	15	15
0	12	4	32	28	1	7	-7	31	33	7	5	-1	18	18
0	14	0	7	2	1	9	0	4	1	7	5	2	82	80
1	1	0	25	26	1	9	1	21	20	7	5	-2	106	107
1	1	1	25	27	1	9	-1	7	1	7	5	-3	16	19
1	1	-1	14	10	1	9	2	11	10	7	5	4	63	62
1	1	2	72	65	1	9	3	46	47	7	5	-4	87	86
1	1	-2	38	40	1	9	-3	42	42	7	5	-5	12	11
1	1	3	13	16	1	9	-4	4	3	7	5	-6	27	25
1	1	-3	27	24	1	9	5	29	29	7	7	0	54	55
1	1	4	29	27	1	9	-5	38	37	7	7	1	3	2
1	1	-4	97	99	1	9	-6	8	5	7	7	-1	14	15
1	1	5	19	18	1	11	0	5	6	7	7	2	24	21

d) $Na_{.875}K_{.125}VO_3$ Structure Factors

H	K	L	FO	FC	H	K	L	FO	FC	H	K	L	FO	FC
0	0	2	210	209	1	1	-6	9	10	2	2	-4	48	48
0	0	4	135	135	1	3	0	2	4	2	2	5	61	60
0	2	0	71	70	1	3	1	2	6	2	2	-5	85	85
0	2	1	128	125	1	3	-1	74	75	2	2	6	33	33
0	6	0	132	135	1	3	2	47	45	2	2	-6	12	11
2	0	0	99	96	1	3	-2	39	37	2	4	0	38	39
2	0	-2	108	111	1	3	3	30	31	2	4	1	69	70
2	2	0	74	75	1	3	-3	89	90	2	4	-1	77	78
2	2	-1	182	183	1	3	-4	18	18	2	4	2	42	42
2	2	-3	157	160	1	3	5	42	40	2	4	-2	67	66
3	1	0	123	121	1	3	-5	61	62	2	4	3	35	35
3	1	-1	89	88	1	3	6	19	18	2	4	-3	31	31
4	0	-2	129	127	1	3	-6	6	5	2	4	4	39	40
5	3	1	168	171	1	5	0	71	70	2	4	-4	21	21
5	3	-1	131	133	1	5	1	33	33	2	4	5	34	34
0	0	6	52	52	1	5	-1	30	30	2	4	-5	44	44
0	2	2	21	17	1	5	2	30	28	2	4	-6	31	32
0	2	3	57	57	1	5	-2	10	9	2	6	0	64	65
0	2	4	44	44	1	5	3	34	34	2	6	1	13	13
0	2	5	29	28	1	5	-3	5	5	2	6	-1	12	12
0	2	6	18	16	1	5	4	24	25	2	6	2	30	30
0	4	0	36	40	1	5	-4	11	11	2	6	-2	105	106
0	4	1	119	120	1	5	5	5	5	2	6	3	5	0
0	4	2	94	93	1	7	0	8	8	2	6	-3	3	2
0	4	3	76	75	1	7	1	44	43	2	6	4	25	24
0	4	4	33	32	1	7	-1	30	29	2	6	-4	59	58
0	4	5	46	45	1	7	2	29	29	2	6	5	1	3
0	4	6	37	36	1	7	-2	20	21	2	6	-5	8	7
0	6	1	44	44	1	7	3	29	30	2	8	1	7	9
0	6	2	138	137	1	7	-3	35	35	2	8	-1	65	65
0	6	3	30	30	1	7	4	6	7	2	8	-2	101	100
0	6	4	55	54	1	7	-4	12	12	2	8	2	3	6
0	6	5	13	13	1	7	5	28	27	2	8	-2	8	7
0	8	0	3	1	1	7	-5	11	12	2	8	3	56	55
0	8	1	57	57	1	9	0	7	7	2	8	-3	79	80
0	8	2	29	29	1	9	1	4	5	2	8	4	12	12
0	8	3	37	37	1	9	-1	5	4	2	8	-4	14	15
0	8	4	19	17	1	9	2	5	4	2	10	0	14	14
0	10	0	66	66	1	9	-2	4	1	2	10	1	27	26
0	10	1	25	25	1	9	3	24	24	2	10	-1	37	36
0	10	2	47	46	1	9	-3	6	6	2	10	2	12	11
0	10	3	24	24	1	11	0	4	1	2	10	-2	13	12
1	1	0	19	19	1	11	1	27	24	2	10	-3	24	23
1	1	1	17	16	1	11	-1	8	9	3	1	1	90	89
1	1	-1	9	9	2	0	2	570	10	3	1	2	65	64
1	1	2	44	43	2	0	4	9	11	3	1	-2	17	20
1	1	-2	5	5	2	0	-4	103	103	3	1	3	57	56
1	1	3	21	20	2	0	6	23	22	3	1	-3	57	58
1	1	-3	5	5	2	0	-6	23	24	3	1	4	79	79
1	1	4	31	30	2	2	1	143	139	3	1	-4	82	83
1	1	-4	21	22	2	2	2	67	66	3	1	5	30	30
1	1	5	14	12	2	2	-2	14	16	3	1	-5	32	31
1	1	-5	4	3	2	2	3	79	78	3	1	-6	36	35
1	1	6	10	7	2	2	4	41	42	3	3	0	56	55

H	K	L	FO	FC
6	4	-5	6	7
6	4	-5	7	7
6	6	0	11	12
6	6	1	5	4
6	6	-1	14	13
6	6	2	7	6
6	6	-1	3	4
6	6	-2	47	48
6	6	3	9	7
6	6	-3	9	9
6	6	-4	8	6
6	6	-5	5	4
6	8	0	2	2
6	8	1	26	26
6	8	-1	11	9
6	8	2	17	16
6	8	-2	5	6
6	8	-3	7	8
6	8	-4	6	6
6	8	-1	3	2
7	1	0	78	81
7	1	1	38	33
7	1	-1	53	53
7	1	2	80	82
7	1	-2	129	128
7	1	3	28	28
7	1	-3	55	56
7	1	4	28	29
7	1	-4	64	64
7	1	-5	38	39
7	1	-6	50	49
7	3	0	19	18
7	3	1	69	70
7	3	-1	90	91
7	3	2	18	19
7	3	-2	15	15
7	3	3	33	32
7	3	-3	66	68
7	3	4	5	3
7	3	-4	10	10
7	3	-5	28	30
7	3	-6	4	2
7	5	0	121	125
7	5	1	10	9
7	5	-1	6	5
7	5	2	63	66
7	5	-2	102	101
7	5	3	10	9
7	5	-3	20	20
7	5	-4	86	86
7	5	-5	18	18
7	7	0	48	48
7	7	1	17	16
7	7	-1	31	31

H	K	L	FO	FC
7	7	2	21	22
7	7	-2	33	33
7	7	3	29	28
7	7	-3	41	40
7	7	4	12	10
7	7	-4	5	5
7	7	-1	23	22
7	7	2	30	33
7	7	-2	25	8
7	7	5	9	4
7	7	-5	32	33
7	7	6	17	17
7	7	-6	16	18
7	9	1	40	40
7	9	-1	41	40
7	9	2	35	37
7	9	-2	13	13
7	9	3	38	38
7	9	-3	55	56
7	9	4	11	10
7	9	-4	46	45
7	9	5	14	14
7	9	-5	20	20
8	2	1	15	15
8	2	-1	9	11
8	2	2	2	3
8	2	-2	17	16
8	2	3	29	30
8	2	-3	21	21
8	2	4	7	7
8	2	-4	11	11
8	2	-1	2	2
8	2	2	4	1
8	2	-2	17	17
8	2	3	6	5
8	2	-3	25	25
8	2	-4	6	6
8	2	-5	2	6
8	2	-1	30	30
8	2	-2	1	3
8	2	-3	28	29
8	2	0	19	19
8	2	1	10	9
8	2	-1	14	13
8	2	2	22	21
8	2	-2	61	58
8	2	3	15	14
8	2	-3	19	20
8	2	-4	33	33
8	2	-5	25	24
8	2	-6	41	41
8	2	0	18	19
8	2	1	47	49
8	2	-1	82	84

H	K	L	FO	FC
9	3	2	9	7
9	3	-2	92	92
9	3	3	24	23
9	3	-3	59	59
9	3	4	15	16
9	3	-4	9	11
9	3	5	10	11
9	3	-5	4	2
9	5	1	22	21
9	5	-1	4	5
9	5	2	45	45
9	5	-2	12	12
9	5	3	27	28
9	5	-3	27	27
9	5	4	21	20
9	5	-4	38	37
9	5	5	51	51
9	5	-5	78	78
9	7	0	70	67
9	7	-1	47	45
9	7	1	16	17
9	7	-1	32	31
9	7	2	20	20
9	7	-2	29	30
9	7	-3	39	39
9	7	3	18	17
9	7	-3	8	8
9	7	4	23	23
9	7	-4	49	49
9	7	-5	38	39
9	7	-1	36	34
9	7	-2	21	21
9	7	-3	31	31
9	7	-4	31	32
9	7	0	45	45
9	7	-1	12	11
9	7	-2	25	25
9	7	-3	6	6
9	7	1	20	18
9	7	-1	14	15
9	7	-1	13	9
9	7	-2	11	9
9	7	-3	6	3
9	7	-4	23	23
9	7	3	11	10
9	7	-3	12	11
9	7	-4	1	0
9	7	-1	7	6
9	7	-2	22	22
9	7	0	41	41
9	7	-2	47	39
9	7	-1	65	66
9	7	-2	35	35
9	7	-3	52	51